Classification and properties of nanoparticles

2

Saadbin Khan[a,*] *and M. Khalid Hossain*[b,c,*]
[a]Oklahoma State University, Stillwater, OK, United States, [b]Kyushu University, Fukuoka, Japan, [c]Bangladesh Atomic Energy Commission, Dhaka, Bangladesh

2.1 Introduction

Nanotechnology has been used by craftsmen around the world approximately since 2600 BC, even though it came under limelight fairly recently (Dolez, 2015). The Lycurgus cup (AD 400, Rome), Maya Blue pigment (AD 800, Chichen Itza), Damascus steel sword (AD 300–1700, Middle East), luster pottery (AD 800–1600, Mediterranean region), Deruta ceramics (AD 1450–1600, Umbria, Italy), and air-purifying church windows (medieval Europe) are some of the famous examples of molecular-scale manipulation of matter in ancient empires. Fig. 2.1 depicts the fascinating optical property of the Lycurgus cup that appears different in color depending on where it is being illuminated from (Loos, 2015). Such intricate developments were mostly made on a trial-and-error basis, rather than using any proper understanding of the smaller-scale physics. With technological evolution and miniaturization of domestic and industrial accessories, downsized materials have become more and more desirable. Hence, better insight of atomic- and molecular-level mechanisms of nanostructures has become an absolute necessity. Ever since visionary physicist and Nobel laureate Richard P. Feynman's historic talk to the American physical society in 1959 underlining "There is plenty of room at the bottom" (Feynmann, 2018), researchers have been exploring nanomaterials in order to bridge the gap between bulk- and atomic-scale physics. His prophetic statement indeed turned out to be true as nanotechnology has already reached a dominant position in material engineering, and it is aiming even higher to achieve unbound flexibility and functionalization.

The word "nanotechnology" was first employed by Norio Taniguchi in 1974 in order to highlight the potential of ultra-small elements to achieve ultra-fine precision (Wu et al., 2013). The prefix "nano" generally refers to a size spanning between 1 and 100 nm in the length scale. By this definition, nanoparticles have at least one dimension in the nanometric scale. Typically, quantum dots and 3D nanostructures characterize at the lower and upper threshold of this scale, respectively. Nanoparticles exhibit uniquely enhanced physical, chemical, and biological properties compared to their respective bulk material counterparts (Dolez, 2015). On top of their individual behavior, they can also be used with other materials to acquire unique

[*] Authors contributed equally to this chapter.

Nanoparticle-Based Polymer Composites. https://doi.org/10.1016/B978-0-12-824272-8.00009-9

Fig. 2.1 The Lycurgus cup that appears green (left one) when illuminated from outside, and purple-red (right one) when illuminated from inside.
Reproduced with permission from Loos, M. (2015). Nanoscience and nanotechnology. In *Carbon nanotube reinforced composites* (pp. 1–36). Elsevier. https://doi.org/10.1016/B978-1-4557-3195-4.00001-1.

functionalization for practical uses (Lines, 2008). Hence, in composite physics, nanoparticles are promising candidates for integration into appropriate hosts to form high-performance composite materials (Hoque et al., 2018; Rahman, Hoque, Rahman, Azmi, et al., 2019; Rahman, Hoque, Rahman, Gafur, et al., 2019a, 2019b). This way, the key features from both the host and the nanoparticles are blended together. Therefore, individual properties of nanoparticles require comprehensive exploration to extract the highest benefit in research and innovative studies.

Unique features of nanoparticles result from the three major physical properties that are interrelated. First, nanoparticles have very high specific surface area (area per unit volume), rendering the electronic activity and their interaction with outside influences significant (Sharma, Ganti, & Bhate, 2003). Second, they have high mobility not only in free state, but also in porous media. Finally, nanoparticles exhibit quantum effect due to their comparable dimension with the wavelength of the electron wave function (Cahay, 2001).

Bulk-scale behavior and the atomic or molecular behavior of the same element are different due to their different governing physical laws. Nanoparticles are, by definition, bigger than atoms or molecules that are governed by quantum physics, but way smaller than the bulk objects we encounter all the time that are governed by classical Newtonian physics. At nanoscale, the specific surface area of a particle is so large that it becomes capable of storing more energy, which is not possible at bulk material. Even the space occupied by the electrons floating around at the outermost orbit becomes significant compared to the dimension of the corresponding particle. This

leads to quantum confinement, which triggers drastic changes in the optoelectronic properties. Energy bandgap at this level gets much bigger compared to bulk material (Singh, Goyal, & Devlal, 2018). Such transition in physical behavior is responsible for the enhancements in many properties of the material that can be utilized for the benefit of technology.

Classification of nanoparticles is subject to the context of application or research it is used in. There are numerous criteria that have been taken into consideration by researchers such as origin, morphology, geometry, dimensionality, chemical constituents, toxicity, agglomeration, and so on (Dolez, 2015). Before getting steadfast with a single one out of these, we briefly shed light on some of the major criteria that are used frequently. The most relevant factor to reasonably sustain the flow of information in the current chapter is the chemical structure of particles. Hence, the sections in this chapter are organized in such a way that properties of nanoparticles can be looked upon categorically as a function of their chemical composition. For each category, unique properties are overviewed first with a short detail about their transition from bulk to nanoscale, followed by the individual properties of the most common particles in that category.

2.2 Classification of nanoparticles

A proper classification of the nanoparticles is a prerequisite in order to highlight the category-specific characteristics. This is a bit tricky as there are multiple criteria on which we can establish the classification and there is freedom to choose one that properly accords with the objective of the corresponding research.

2.2.1 According to origin

Based on the origin, nanoparticles can be classified into three major categories:

Natural nanoparticles—As the name suggests, these nanoparticles are available in nature mostly as ultra-fine particles. Common origins in nature are oil, sea waves, sand storms, volcanoes, forest fires, living organisms, crystalline structures, and space (Dolez, 2015).
Incidental nanoparticles—Incidental nanoparticles are emitted as ultra-fine particles as unintended by-products of human controlled processes such as power generation, engine exhaust, material welding, food processing, cigarette smoke, building demolition, and so on.
Engineered nanoparticles—Leveraging modern equipment, extensive variety of chemical catalysts, and novel synthesis techniques, nanoparticles are now engineered artificially in order to provide enhancement to targeted characteristics that suit certain functionalities.

2.2.2 Dimensional classification

Fundamentally, all nanoparticles have at least one dimension inside the nanometric size range (between 1 and 100 nm). They are categorized into four types based on dimensionality described as follows and illustrated in Fig. 2.2 (Dolez, 2015).

- Zero-dimensional nanoparticles—If all external dimensions of a nanoparticle are at nanoscale, it is classified as zero dimensional (0D). Quantum dots (QD) are the most widely used

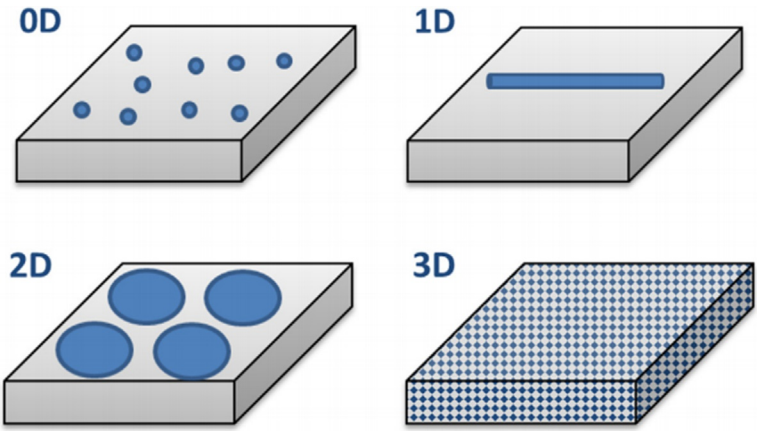

Fig. 2.2 Classification of nanoparticles based on their dimensionality.
Reproduced with permission from Dolez, P. I. (2015). Nanomaterials definitions, classifications, and applications. In *Nanoengineering* (pp. 3–40). Elsevier. https://doi.org/10.1016/B978-0-444-62747-6.00001-4.

0D nanoparticles having crucial application in electronics because of their enhanced optical and transport properties due to the highest level of quantum confinement. Individual molecules also belong to this category when they are essentially isolated from each other to be considered as nanoparticles.

- One-dimensional nanoparticles—Nanoparticles comprising only one dimension outside of the nanometric size range and the other two dimensions at nanoscale range are called one-dimensional (1D). These particles play a vital role in the construction of nanowires, nanotubes, nanorods, nanobelts, etc. and work as one of the major building blocks of hierarchical nanostructures.
- Two-dimensional nanoparticles—Two-dimensional (2D) nanoparticles have two dimensions outside of the nanometric size range. These particles exhibit characteristics of thin films, nanosheets, or nanocoatings. They have extensive applications in nanostructured devices such as sensors and nanoreactors (Hossain, Ahmed, Khan, Miah, & Hossain, 2021). Carbon nanotubes (CNT) are popular examples of such nanoparticles that exhibit two-dimensional structure locally. They are composed of a 2D layer of graphite rolled to form a tubular structure.
- Three-dimensional nanoparticles—Three-dimensional (3D) nanoparticles display nanoscale feature internally even though none of the three external dimensions are at nanoscale. Fibrous, multilayer, and polycrystalline materials as well as some powders belong to this category. They are structurally composed of lower-dimensional nanoparticle elements as building blocks. 3D nanoparticles are of extreme importance having a wide range of applications in modern nanotechnology. Two such promising particles are fullerenes (also known as carbon 60) and dendrimers.

2.2.3 Based on chemical composition

Based on the chemical composition, nanoparticles can be classified into several categories.

- Metallic nanoparticles—Because of the superior physical properties, pure metal nanoparticles are one of the oldest and most popular nanoparticles used by scientists. In modern times, they are being deployed into diverse applications most significantly in biomedical sector, i.e., for targeted delivery of bioactive drugs, as vehicle for gene delivery, biosensors, imaging, as antimicrobial agents, and so on (Hossain, Khan, & El-Denglawey, 2021). Most common metal nanoparticles include gold, silver, copper, iron, lead, cadmium, cobalt, and platinum nanoparticles. Oxides of metals are more chemically stable than metals as the free electrons get occupied in the bond with oxygen. Depending on the molecular structure, different oxides exhibit different characteristics either of a conducting metal, a semiconductor, or an insulator. Flexibility in tuning favorable properties makes them the most widely manufactured nanoparticles having diverse applications such as biochemical sensing, alkaline and lithium ion battery cells, solar absorbers and energy harvesters, piezoelectric, ferroelectric, and magnetic devices, lasers, superconductors, etc. Based on their cationic constituent and their electrochemical properties, these oxide nanoparticles can be further categorized into different subsets such as metal oxide nanoparticles, semiconductor nanoparticles, ceramic nanoparticles, etc. The most commonly used oxide nanoparticles include zinc oxide (ZnO), iron oxides (FeO, Fe_2O_3, Fe_3O_4), aluminum oxide (Al_2O_3) (Manzoor, Ashraf, Tayyaba, & Hossain, 2021), silica (SiO_2), copper oxide (CuO), magnesium oxide (MgO), nickel oxide (NiO), titanium oxide (TiO_2), cerium oxide (CeO_2), and zirconium dioxide (ZrO_2).
- Semiconductor nanoparticles—Semiconductor materials have electrical conductivity in between conductors and insulators. They have electron bandgap less than that of insulators and more than that of conductors. Even though there is no strict quantitative definition; generally, materials with a bandgap of 3.5 eV or less are considered semiconductors. They exhibit drastic changes in their property when reduced to nanoscale level due to their large surface area and quantum size effect in play at that scale. Artificially engineered one-dimensional semiconducting crystal can be further categorized as quantum dots (QD). Just by controlling the size of specific QDs, one can fine-tune their physical, optical, and electrical properties such as wide energy band gap, spectral photo response from IR to UV covering the entire visible light region, narrow emission spectra, etc (Hossain et al., 2021). Such alterable properties make semiconductor nanoparticles very promising candidates for a wide range of industrial, electrical, and biomedical applications, including nanoscaled light-emitting devices, integrated circuits, laser technology, biological sensing, labeling, and imaging, etc. Based on the position of the constituent elements of the compound in the periodic table, semiconductor nanoparticles can be classified into different categories. The following list shows the major categories:
  - IV semiconductor—silicon (Si), germanium (Ge)
  - II–VI semiconductors—ZnS, ZnO, CdS, CdSe, CdTe
  - III–V semiconductors—GaN, GaP, GaAs, InP, InAs
  - Nanoshells

Advancements in material physics have allowed the formation of other semiconducting compounds composed of a combination of different groups outside of the above categories, including some common metal oxides such as ZnO, TiO_2, and SnO_2. Core-shell nanomaterial or nanoshell is essentially composed of two or more different materials, out of which at least one material forms the core at nanoscale encapsulated by another material acting as the shell. The core, the shell, or both can be made of semiconducting material. Nanoshells can be of two major types, namely, oxide nanoshells and metal nanoshells. Oxide nanoshells have a hollow core with oxide

coating (i.e., hollow silica nanoshell), while metal nanoshells are composed of a dielectric core with metal coating (i.e., gold and silver nanoshells) (Dahman, 2017; Nayak et al., 2017).

- Carbon-based nanoparticles—Due to the four valance electrons in its atomic structure, carbon is one of the few elements capable of forming multiple allotropes that are structurally different from each other. This special capability of carbon-based nanotechnology with a family of allotropic particles each having its own unique advantage. Carbon-based nanostructures include but are not limited to diamond, graphene, fullerene, carbon nanotubes (CNT), carbon nanofibers (CNF), carbon black, and carbon dots.
- Ceramic nanoparticles—As the name suggests, ceramic nanoparticles are composed of inorganic solids (i.e., oxides, carbides, phosphates, and carbonates of both metals and metalloids (Diao, Gall, & Dunn, 2003)) at nanoscale length scale. They show porous characteristics providing them protection from physical degradation. They were discovered in the early 1980s using a process named "sol-gel." Since then, ceramic nanoparticles have been popular especially because of their superior mechanical properties and high-temperature resistance.
  - Oxide-based ceramic nanoparticles—silica (SiO_2), alumina (Al_2O_3), titania (TiO_2), zirconia (ZrO_2), etc.
  - Nonoxide-based ceramic nanoparticles—silicon carbide (SiC).
- Lipid-based nanoparticles—lipid-based nanoparticles represent a clinically advanced class of systems specialized as nanocarriers. The most vital reason why these particles garnered wide attention is their application in cancer treatment and drug delivery. Unique chemical structure makes them versatile with the capability of transporting hydrophobic, hydrophilic, and amphiphilic molecules. Moreover, they exhibit high biocompatibility and almost no toxicity. Significant research is still ongoing to engineer their functionality with help of novel as well as modified composition. Based on the architecture, lipid-based nanoparticles are classified into several types such as solid lipid nanoparticles (SLN), nanostructured lipid carriers, lipoproteins, liposomes, lipid-core micelles, hybrid lipid-nanoparticle complexes (HLNC), lipoplexes, lipid nanoemulsions, etc.
- Polymeric nanoparticles—polymeric nanoparticles refer to colloidal structures comprising of active compounds entrapped within or surface-adsorbed onto polymeric core. They are promising drug carriers because of their biocompatibility, controlled releasing profile, and non-toxic and non-immunogenic properties. Based on the morphological structure, polymeric nanoparticles can be further classified into either nanocapsules or nanospheres. The distinguishing factors between these two types are: bioactive compounds are chemically integrated within polymer matrix in nanospheres, while they are entrapped within the polymeric shell in nanocapsules.

2.2.4 Based on morphology

Many applications of nanoparticles require a specific range for size or shape. This mandates another classification based on the morphology. Various shapes of nanoparticles include: spherical, triangular, cubic, hexagonal, oval-shaped, prism-shaped, rod-like, tube-like, helical, and so on (Gatoo et al., 2014). Also, they can have different intrinsic crystal structures such as simple cubic, body- or face-centered cubic, icosahedron, decahedron, etc. (Sweet, Chessher and Singleton, 2012).

2.3 Different properties of nanoparticles

Properties of a material change drastically when they are downsized to nanoscale level. Methods and conditions used to synthesize such nanoparticles largely influence these properties. Also, they are quite tunable mostly by controlling their morphology. In the following sections of this chapter, we explore those properties in detail. To keep this exploration systematic for the reader, we choose the classification based on chemical composition and discuss the properties of nanoparticles in each class. We first shed light on the general properties of each class and then discuss the unique properties of the most common nanomaterials in that class. The whole set of different properties of a nanoparticle are divided into several subsets as follows.

2.3.1 Morphological properties

Morphology refers to the size, shape, and crystal structure of nanoparticles. At nanometric length scale (1–100 nm in general), the particle diameter is at the same level of the wavelength of its motion so that their behavior is governed by quantum-level physics. Because of the small dimensions of nanoparticles, they have very high mobility in free state. Also, in favorable circumstances, they can often reach even submicron-scale pores. Such attributes particularly benefited biomedical sector leading to novel methods for cellular-level treatment and targeted drug delivery (Hossen et al., 2019; Khan et al., 2022). Specific surface area (i.e., ratio of surface area to volume) of a nanoparticle is generally larger compared to their bulk counterpart to accommodate enhanced properties. Furthermore, nanoparticles can be found in several crystal structures that define their nanoscale behavior to a significant extent. One material can be found as multiple polymorphs exhibiting different structure.

2.3.2 Surface effect

Most of the nanoscale particles are structurally unique because of their significantly higher ratio of surface area to volume. This is because the bonding configuration of atoms lying on the surface of a nanomaterial is very different compared to that of the atoms of corresponding bulk material. The surface atoms of the crystal lattice at nanoscale constitute a quite considerable fraction of the total number of atoms in the lattice itself (Khairutdinov, 1998). This surface effect partially accounts for unexpected variations in mechanical and physical properties in nanoparticles compared against their bulk nature. At such small length scale, local atomistic formation becomes hugely influential and the properties become sensitive to the size of the particle and crystal structure. More specifically, atoms in nanoscale always look for reformations to acquire minimum energy configuration, which understandably results in unusual surface stress (Diao et al., 2003).

2.3.3 Quantum size effect

The electronic structure in a bulk material gets changed when reduced to nanoscale. Due to the extreme confinement of electrons and holes inside small crystalline structure, the discrete energy band levels get quantized, which consequently affects the

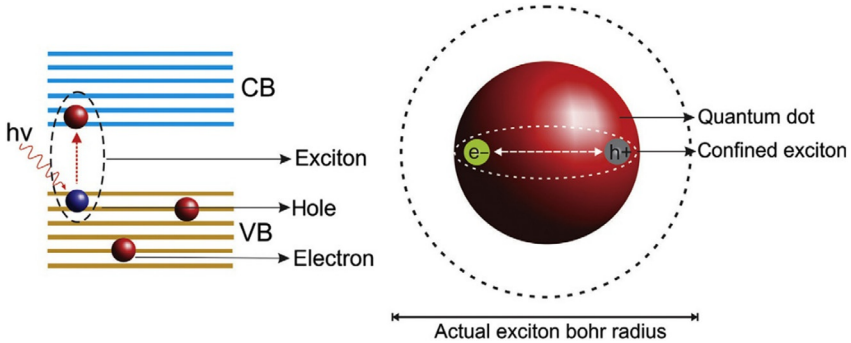

Fig. 2.3 Exciton bound between valence and conduction bands (left one), and a visual comparison between exciton radius and the radius of quantum dot (right one). Reproduced with permission from Sumanth Kumar, D., Jai Kumar, B., & Mahesh, H. M. (2018). Quantum nanostructures (QDs): An overview. In *Synthesis of inorganic nanomaterials* (pp. 59–88). Elsevier. https://doi.org/10.1016/B978-0-08-101975-7.00003-8.

optical, electrical, and magnetic behaviors of nanoscaled materials. This effect can be explained only by exploring physics at a quantum level, instead of the Newtonian physics on bulk material, which is merely a cumulative or averaged exhibition of the quantum-level physics. Some examples of drastic alteration of properties at nanoscale are as follows: Opaque copper becomes transparent, inert platinum shows catalytic behavior, aluminum becomes combustible, gold's melting point falls down to room temperature, silicon turns to be electrical conductor, etc.

Excitons play the crucial role in quantum effect or confinement. An exciton is referred as the state of the excited electron that is bound to the hole it leaves behind in the valence band (VB) while absorbing energy to step up to conduction band (CB). This unique state of exciton is a consequence of the diameter of the quantum dots being smaller than the exciton Bohr radius, which is an inherent property of material. This whole idea is articulated well by Kumar et al. in light of the behavior of nanocrystal quantum dots as illustrated in Fig. 2.3 (Kumar, Kumar, & Mahesh, 2018).

Based on strength, quantum confinement can be categorized into weak, moderate, and strong confinement. Metric for such categorization is the crystallite radius compared with the Bohr radius. Energy shift in different strength regimes is quantified using several parameters such as bulk exciton Bohr radius, electron and hole Bohr radii, mass of the exciton, and the radius of crystallite as described in Suresh (2013).

2.3.4 Other physical properties

Nanoparticles exhibit excellent enhancement in physical properties compared to corresponding bulk elements. The following are the most pronounced properties listed briefly that will be elaborated further in later sections.

- Mechanical properties—In general hardness, ductile and elastic strengths, adhesion, friction, etc. are included in mechanical properties.

- Thermal properties—Melting and boiling points of a bulk material are, in general, independent of morphology. However, such property in smaller-scale particles exhibits significant dependence on dimension. Based on numerous thermodynamic models over the past hundred years, the melting point of nanoparticles has been reported to decrease sharply below a certain size (Nanda, 2009). For instance, Fig. 2.4 illustrates the melting point depression in several metal nanoparticles with downsizing (Qi & Wang, 2004). Moreover, due to the large specific surface area, thermal conductivity and coefficient of thermal expansion are expected to be higher in nanoparticles compared to bulk elements.
- Optical properties—Color, refractive index, reflection capabilities, light penetration, absorption abilities, etc., of nanoparticles are referred as optical properties.
- Electrical properties—Electrical properties can be characterized by conductivity, resistivity, and semiconducting behavior.
- Chemical properties—Chemical properties include chemical stability, reactivity, redox potential, flammability, resistance to corrosion, interaction with water, lipid, or other solvents (i.e., hydrophilicity, hydrophobicity, lipophilicity, etc.), colloidal suspension, diffusion, and settling characteristics.

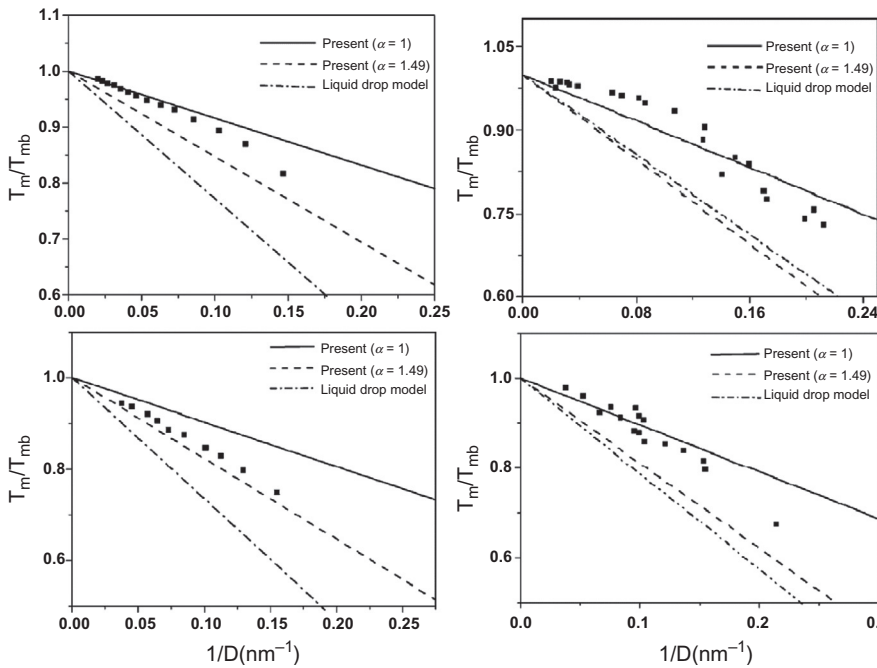

Fig. 2.4 Variation of the melting temperature of Sn (top left), Pb (top right), In (bottom left), and Bi (bottom right) nanoparticles as the function of the inverse diameter. Here, the *solid square symbols* denote the experimental values, and α represents the dimensionless shape factor defined by the ratio of the surface area of a particle to the equivalent spherical nanoparticle of same volume.

Reproduced with permission from Qi, W. H., & Wang, M. P. (2004). Size and shape dependent melting temperature of metallic nanoparticles. *Materials Chemistry and Physics*, *88*(2–3), 280–284. https://doi.org/10.1016/j.matchemphys.2004.04.026.

- Magnetic properties—Only a specific group of nanoparticles exhibit magnetic properties that are characterized by their ferro- and superparamagnetic behavior and their transition from one to other at nanoscale.
- Antimicrobial properties—In biomedical applications, interaction of certain nanoparticles with bacteria, viruses, and other microbial agents to withstand their growth is very important.
- Toxicological properties—To measure both environmental and biocompatibility, toxicity assessment of nanoparticles is necessary.

2.4 Properties of metallic nanoparticles

Highly conductive metal and metal oxide nanoparticles are prepared by chemical, electrochemical, or photochemical syntheses. Owing to their high surface energy and strong adsorption of small molecules, they are applied in bioanalysis for the detection and imaging of biomolecules. Common properties exhibited by metallic nanoparticles include superparamagnetism, catalytic behavior, superior mechanical strength and optical properties, and so on (Li, Silvers, & Samy El-Shall, 1996). Moreover because of the quantum size effect, melting points and adsorptive properties of these nanoscaled particles can be easily modulated in order to serve specific engineering purpose.

2.4.1 Localized surface plasmon resonance (LSPR)

When an external electromagnetic field is applied on a plasmonic material such as a metal body, the free conduction electrons on its surface interact with the incident photon and initiate a collective resonant oscillation along the direction of the electric field of the incident photon. This resonance is dependent on the size and the shape of the material particles and manifested as an optical effect widely known as surface plasmon resonance (SPR). In a bulk body, this oscillatory phenomenon is characteristically delocalized and propagating. Kosuda, Bingham, Wustholz, and Van Duyne (2011) illustrate SPR in a metal-dielectric interface as in Fig. 2.5A. But in significantly downsized materials, this effect is localized or confined to small region, such as in nanoparticles. This is attributed to the dimension of the nanoparticles being even smaller than corresponding SPR wavelength. Zalevsky et al. describe such localized SPR (LSPR) when subjected to external electric field as in Fig. 2.5B where the free electron cloud is displaced producing uncompensated charges near the surface of the metal nanosphere (Kosuda et al., 2011). LSPR in metal nanoparticles results in very strong scattering and absorption properties, which allows them to be effectively visualized with conventional microscope. Owing to the added advantage of favorable biocompatibility, these plasmonic particles have important applications particularly in the biomedical sector such as in plasmonic photothermal therapy and laser treatment of tumor with minimal damage to healthy tissues (Kim & Globerman, 2017).

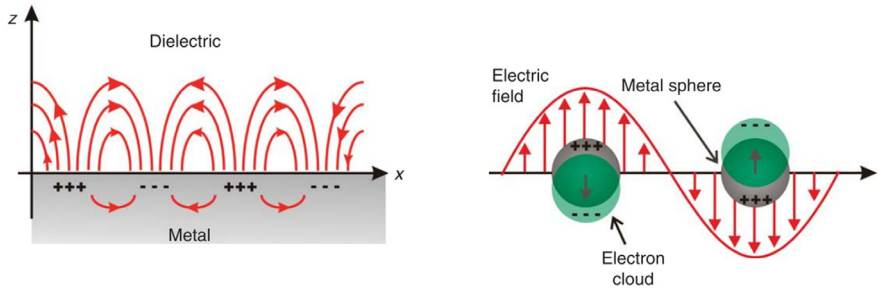

Fig. 2.5 Schematic of SPR in a metal-dielectric interface (left one), and LSPR subject to external electric field (right one).
Reproduced with permission from Kosuda, K. M., Bingham, J. M., Wustholz, K. L., & Van Duyne, R. P. (2011). Nanostructures and surface-enhanced Raman spectroscopy. In *Comprehensive nanoscience and technology* (pp. 263–301). Elsevier. https://doi.org/10.1016/B978-0-12-374396-1.00110-0.

2.4.2 Ferromagnetism and superparamagnetism

Some metals and metal oxide nanoparticles (i.e., iron and iron oxides) are classified as magnetic particles as their properties can be manipulated using magnetic fields. Often such particles at nanoscale are coated with surfactants, polymers, silica, etc., in order to enhance their functionality by improving reactivity. With proper surface functionalization, such particles are widely used in biomedical applications such as cancer treatment, remote heating of tumor cells without damaging healthy tissue, magnetic drug delivery (Anik, Hossain, Hossain, Ahmed, & Doha, 2021), and magnetic resonance imaging (MRI). Such magnetic properties are, in general, referred as ferromagnetism (Mahfuz, Hossain, Khan, Hossain, & Anik, 2022).

However, when the size of these nanoparticles is sufficiently small (diameter not more than 10–20 nm), they exhibit superparamagnetism, which is a rare characteristic of ferro- or ferrimagnetic material particles. Huber (2005) shortly explain this phenomenon on the way to discuss properties of iron nanoparticles. The bottom line is that in the absence of an external magnetic field, superparamagnetic nanoparticles exhibit zero net magnetization unlike a ferromagnetic particle as illustrated in Fig. 2.6 (Alcantara & Josephson, 2012). More specifically, when the thermal relaxation time between flips of magnetic moment is too small compared to the required observation time, the average magnetization value appears to be zero. Magnetic status of such particle is turned on under the influence of a magnetic field, and the magnetic moment is aligned with the applied field. As this phenomenon essentially balances the magnetic and thermal energy, below a certain "blocking" temperature, superparamagnetism vanishes and coercivity takes over. Coercivity is a metric to quantify the resistance of a magnetic particle to change in magnetization under an external field. Mathematical aspects of size-dependent coercivity and transition from ferromagnetism to superparamagnetism are further explored in several works in early 21st century (Alcantara & Josephson, 2012).

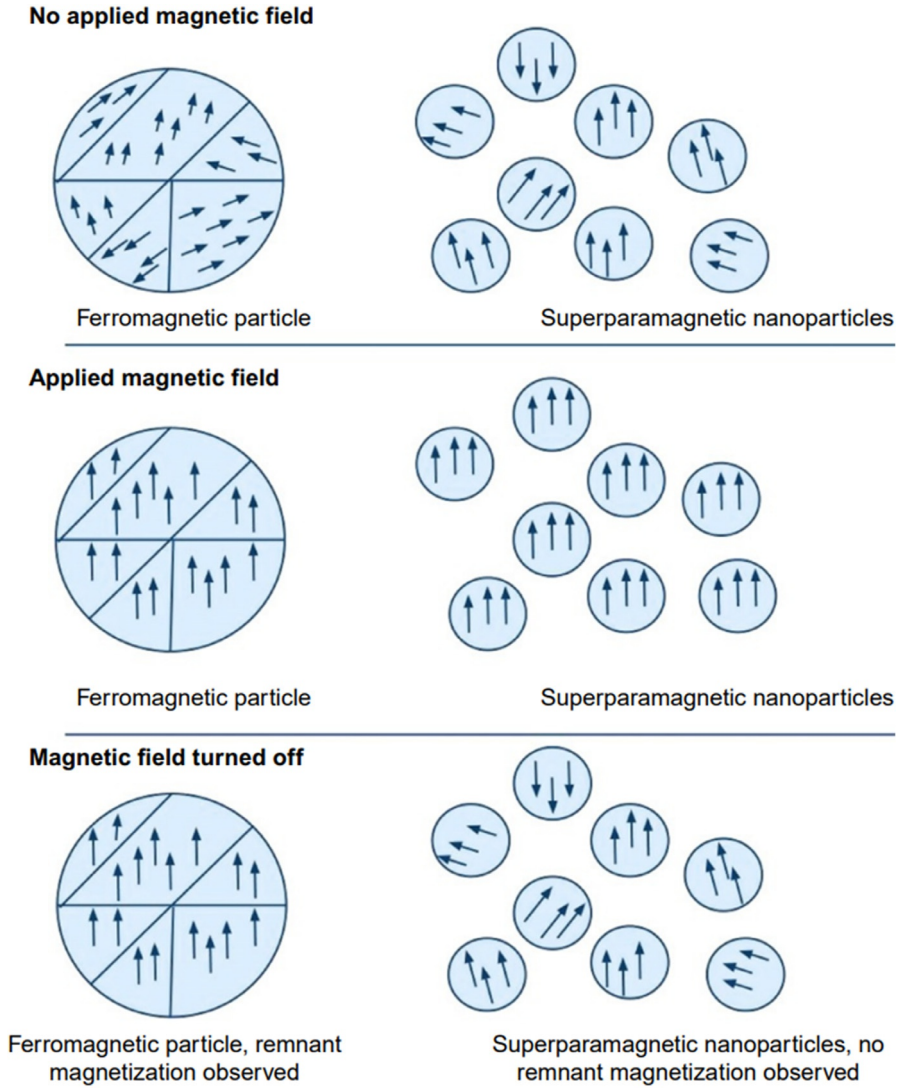

Fig. 2.6 Comparison of magnetic moment alignment in ferro- and superparamagnetic particles when magnetic field is not applied, not applied, and turned off.
Reproduced with permission from Alcantara, D., & Josephson, L. (2012). Magnetic nanoparticles for application in biomedical sensing. In *Frontiers of nanoscience* (1st ed., Vol. 4, Issue 1, pp. 269–289). Elsevier Ltd. https://doi.org/10.1016/B978-0-12-415769-9.00011-X.

2.4.3 Properties of gold nanoparticles

Gold is the most ancient and most prominently used metal nanoparticles. Since the start of extensive study of nanoscaled gold particles in 1850, they have been popularly used because of their superior physical properties. More importantly, these properties can be flexibly tuned by controlling their morphology (both size and

shape), solvent, surface ligand, temperature, etc. Compared with other plasmonic particles, localized SPR is more pronounced in spherical gold nanoparticles resulting in strong radiative, absorption, and scattering properties. Absorption peak at 400–550 nm depending on the particle size and great fluorescence quenching ability is reported, which make gold nanoparticles popular in bio-imaging, probing, colorimetric sensing, and sensor fabrication (Yeh, Creran, & Rotello, 2012). In scanning electron microscope (SEM), they are used for coating the sample in order to acquire high-quality image by enhancing the electronic stream. Adding to that, the large specific surface area and high electron density at nanoscale make gold particles a popular vehicle to carry therapeutic molecules, targeted drugs, genes, and targeting agents on their surface. Particularly in tumor and cancer treatment, gold nanoparticles have become a promising tool. Photocatalytic and redox properties of gold nanoparticles suit to be used for selective oxidation and targeted inhibition of certain reactions in electrochemical devices. They are usually chemically stable, and low acute toxicity has been reported.

2.4.4 Properties of silver nanoparticles

Silver nanoparticles have numerous applications in biomedical devices, medicines, highly conductive composites, cosmetics, textile industries, and so on because of their interesting physical properties. They exhibit effective SPR, strong absorption peaking near 400 nm, and tunable scattering property at larger wavelength, all of which are suitable for bio-imaging, molecular labeling, and enhanced optical spectroscopy. For a long time, nanoscaled silver is considered a very popular biomaterial with antimicrobial activity described briefly by Zhang, Liu, Shen, and Gurunathan (2016). Their antibacterial behavior is popularly used for minimizing bio-fouling. They have recently performed well against HIV virus and for apoptosis of cancer cells. Moreover, their antiinflammatory activity is suitable to heal wounds. Toxicity of silver nanoparticles is majorly dependent on their morphological status and surface charge. Negatively charged silver nanoparticles are reported to be less toxic compared to positively charged particles (El Badawy et al., 2011).

2.4.5 Properties of copper nanoparticles

Copper nanoparticles have garnered attention, because they are comparatively cheap, chemically stable, and can be easily synthesized (Basher et al., 2019). They exhibit high melting point, very high thermal and electrical conductivity, great ductile strength, and strongly localized SPR. They are used to be applied as a coloring agent in ancient times. Even now, they are viable alternative to noble metal nanoparticles (gold and silver) as pigment constituents used in inkjet printing. Due to catalytic and antibacterial characteristics, they are widely used in biomedical and pharmaceutical applications. However, some adverse biological effects of copper nanoparticles on the embryogenesis along with cellular toxicity and DNA damage have been reported (Zhang et al., 2018).

2.4.6 Properties of aluminum nanoparticles

Aluminum is the most abundant metallic material found in earth's crust. It is very light, ductile, great conductor of heat and electricity, and gains chemical stability by forming an oxide layer while exposed to environment. Owing to their catalytic activity and high energy release, aluminum nanoparticles are used in rocket fuel as powder to improve combustion speed and stability. They exhibit a broad optical absorption band, and hence, the LSP resonances can be tuned ranging from UV to NIR by controlling their morphology. Adding to that, their high radiative efficiency (Temple & Bagnall, 2011) makes them suitable to be used in photovoltaic solar cells.

2.4.7 Properties of iron nanoparticles

Iron is one of the most abundant elements in nature, and its nanoparticles exhibit good thermal and electrical conductivities along with one of the strongest magnetic nature among all magnetic nanoparticles (Rubel & Hossain, 2022). Even though iron nanoparticles show SPR as expected from a metal nanoparticles, such optical behavior has not been under too much scrutiny compared to their unique magnetic properties that have crucial applications in memory tape, magnetic data storage, and magnetic resonance imaging (MRI). To start with, they exhibit superparamagnetism when their diameter goes below 10 nm. Bødker, Mørup, and Linderoth (1994) reported that iron nanoparticles with a diameter of about 2 nm exhibit magnetic properties similar to bulk α-Fe and magnetic anisotropy energy constant goes up with downsizing. Such downsizing also invokes a pronounced reactivity in the presence of oxygen or water (i.e., readily forms oxides), which is comparatively weak in the bulk material. Such alterations in the chemical and magnetic behavior are attributed to the surface effects, more specifically, to the added energy stored in the surface with higher specific area at nanoscale. For better functionalization as magnetic nanoparticles, inorganic oxygen barriers (such as gold) can be used as nonreactive shells (Anik et al., 2021). Furthermore, they have good catalytic property in an inert or nonoxidizing environment to make and break carbon-carbon bonds.

2.4.8 Properties of iron oxide nanoparticles

There are 16 identified oxides of iron having different chemical combinations of iron and oxygen. They can generally be naturally found or industrially produced. The most abundant forms that are broadly found in nature are hematite (α-Fe_2O_3), maghemite (γ-Fe_2O_3), and magnetite (Fe_3O_4).

Iron oxides are the most extensively explored magnetic nanoparticles. When particle size is smaller than 10 nm, they exhibit superparamagnetic behavior, which makes them extremely important for various biomedical applications. They gained attention particularly due to their compatibility as contrast agent for magnetic resonance imaging (MRI) and as nanocarrier for bio-elements such as drug, protein, therapeutic gene, etc. Even though magnetic properties of nanoparticles are crucial,

toxicity is often one of the limitations that render major magnetic elements incompatible for biomedical use. In that sense, it is more feasible to use magnetic properties of iron oxides as they do not have oxidization issues like nickel (Ni) and cobalt (Co). Similar to metal nanoparticles and other magnetic oxide particles, iron oxide also exhibits light scattering and absorption properties that are subject to the size of the particle.

2.4.9 Properties of platinum nanoparticles

Even though platinum is one of the most expensive metals around, superior chemical and optical properties of its platinum nanoparticles are of rising interest in industrial and biomedical applications. Crystal structure of platinum is face-centered cubic, and its nanoparticles are, in general, suspended in aqueous solution to form brownish-red or black nanofluid. They exhibit superior thermochemical stability, corrosion resistance, and significant catalytic activity. Such behavior renders them suitable to be used in catalytic converters, hydrogen peroxide (H_2O_2) decomposition, nitric acid production, proton-exchange membrane fuel cells (PEMFC) (Reddington et al., 1999), pollutant reduction, and so on. Furthermore, in room temperature, carbon-coated platinum nanoparticles exhibit ferromagnetic behavior. They are often co-used with other metallic particles to form ultra-efficient alloys, or as dopants with semiconductor nanoparticles (i.e., with ZnO, TiO_2) to improve thermo-electrical properties and oxidation activity. Localized SPR exhibited by platinum nanoparticles peaks in the UV region at about 215 nm. Toxicological study of platinum nanoparticles is still underway. However, some amount of cytotoxicity and genotoxicity due to more negative zeta potential of the particles have been reported (Elder et al., 2007), even though they exhibit an enhanced antibacterial activity. Enhanced radiation efficiency in cancer therapy has been reported compared to other plasmonic nanoparticles (Porcel et al., 2010). Other biomedical applications owing to the favorable properties of platinum nanoparticles are targeted drug delivery, photothermal therapy, biosensing, and imaging.

2.4.10 Properties of lead nanoparticles

Lead is a dense yet malleable metal. Nanoparticles of lead are, in general, black spherical powder. When deployed in applications as nanostructured thin films, lead nanoparticles are reportedly prone to oxidation and sensitive to water and humid ammonia (Bochenkov, Zagorsky, & Sergeev, 2004). Due to the optical and redox properties, they have potential applications in electron microscopy for real-time imaging.

2.4.11 Properties of cobalt nanoparticles

Pure cobalt nanoparticles are gray or black powders having relatively small amount of applications (Liu et al., 2015). Importantly, they show good magnetic properties, making them suitable for imaging, sensing, and targeted delivery of biological molecules

and agents. Toxicity and biological properties of cobalt nanoparticles are subject to application. For instance, Liu et al. explained such properties in light of the effect on osteoclast-like cells (Liu et al., 2015).

2.4.12 Properties of copper oxide nanoparticles

Copper oxide (CuO) is chemically composed of 80% copper and 20% oxygen, and at nanoscale level, its properties are highly dependent on synthesis method, temperature, material composition, and most importantly morphology. They are spherical with 1–30 nm in diameter having high specific surface area. Crystal structure is monoclinic where the copper atom is bonded with oxygen in a rectangular configuration. Morphology highly influences the other properties of CuO (Saha et al., 2018). Major properties of these popular magnetic nanoparticles are illustrated in light of their synthesis method and biomedical applications by Grigore, Biscu, Holban, Gestal, and Grumezescu (2016). CuO nanoparticles with a dimension of a few nanometers are reported to exhibit weak ferromagnetic behavior (Zhang et al., 2014), while another study (Bisht, Rajeev, & Banerjee, 2010) reported the absence of conventional zero field cooled (ZFC) (Joy, Kumar, & Date, 1998) magnetization. CuO nanoparticles show antimicrobial properties that are exploited in textile industries and in hospitals to prevent bacterial infection. Even though there are studies (Verma & Kumar, 2019) that have been recently justifying the potential of CuO nanoparticles in biomedical applications because of their sensing and therapeutic features, there is intense debate on the toxicity of these particles. Some investigations report them to be highly toxic as they may cause DNA damage and dose-dependent cytotoxicity while used internally (Fahmy & Cormier, 2009). On the bright side, CuO nanoparticles also show a catalytic property that is utilized in nonbiomedical applications such as with rocket propellants in order to improve burning rate. Moreover, they show excellent redox potential and stability in solutions. Optical properties of CuO nanoparticles can be characterized by UV-Vis absorption spectroscopy. Transmission and absorption bandwidths vary with temperature as well as synthesis method. Similar to metal nanoparticles, CuO nanoparticles also exhibit superior electrical conductivity. This property is reported to be increased with synthesis temperature and concentration in case of aqueous solution (Dimens, 2015; Zhang et al., 2014).

2.5 Properties of semiconductor nanoparticles

Semiconducting materials exhibit electrical conductivity higher than of a conductor and lower than of an insulator. Even though there are certain sets of such materials that are prevalently used in nanotechnology, there are some common characteristic properties specifically distinguishing them from other nanomaterials. We first shed light on those common properties, then move on to discuss individual semiconductor nanoparticles.

2.5.1 Widened electronic bandgap

Electronic bandgap refers to the minimum energy required for exciting an electron from the state in the valence band to a state in the conduction band. Width of this gap dictates the size-sensitive tuning of the material properties. Due to the quantum confinement at the nanoscale, most semiconductor nanoparticles exhibit a shift in the bandgap over 1 eV. This shift Δ was first approximated by Brus (1983, 1984) following Coulomb's interaction. The relation can be expressed with respect to bulk bandgap energy as:

$$\Delta = \frac{\hbar^2\pi^2}{2R^2}\left[\frac{1}{m_e^*} + \frac{1}{m_h^*}\right] - \frac{1.8e^2}{\varepsilon}\frac{1}{R'} \tag{2.1}$$

where $\hbar$ = reduced Planck's constant, R = particle radius, m_e^* = effective mass of the electron, m_h^* = effective mass of the hole, ε = dielectric constant of the semiconductor, and R' = a function of R and ε averaged over the energy wave. This equation suggests that the bandgap shift is approximated to be inversely proportional to the square of particle radius and effective mass. Malik, O'Brien, and Revaprasadu (2000) explain this phenomenon and its consequences in more detail. The bottom line is that when semiconductor particles are sufficiently small (i.e., at nanoscale), energy spacing between two quantized levels is significantly widened, which provides them a unique thermal stability. This effectively eliminates the necessity of safety measures (i.e., excess wires, complex cooling system) in order to withstand abrupt temperature rise. Therefore, electronic control of complex systems undergoing high-temperature processes such as aircraft engines can attain improved reliability. Further enhancement in properties of these nanomaterials with wide bandgap can be triggered by properly doping them with suitable material at specific temperatures.

There are two types of bandgaps in semiconducting materials, namely, direct and indirect bandgap. When the maximum energy state in the valence band, E_v,aligns with the minimum energy state of the conduction band, E_c at a certain crystal momentum, k, such semiconductors are referred as direct bandgap semiconductors. Examples include InAs, GaAs, amorphous silicon, etc. On the other hand, if the two energy states are misaligned because of the difference in the crystal momentum, then they are indirect bandgap semiconductors. AlSb, Ge, and crystalline silicon are common examples of such material. Fig. 2.7 illustrates the energy transition from E_v to E_c in a very simple manner. It is observed that electrons in a direct bandgap material can emit photons directly without any other intermediate transition, whereas electrons in an indirect bandgap material necessarily need to go through a phonon-induced transition before they can emit photons.

2.5.2 Absorption spectrum

When the frequency of the incident light is in resonance with the energy gap of the material and the selection rule (Stanton, 1973) for quantum-state transition is satisfied, photon is absorbed. Direct bandgap semiconductors exhibit a well-defined excitonic

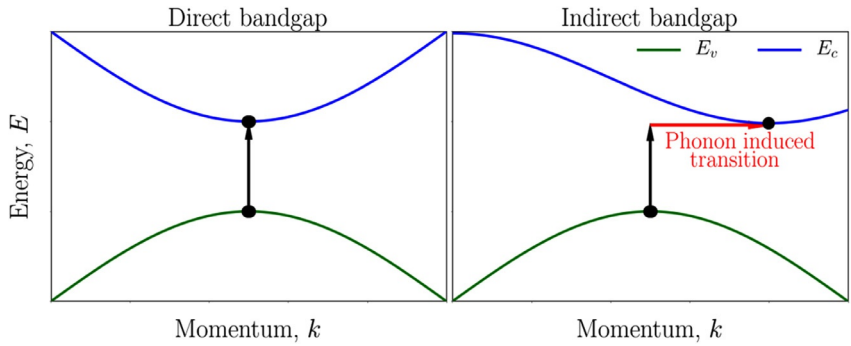

Fig. 2.7 Energy transition in direct and indirect bandgap semiconductors.

peak when the absorption spectrum is observed. Also, due to quantum confinement, blue shift (i.e., shift of the absorption edge to high frequency range) is evident as a result of downsizing in the nanoparticles. This effect is most clearly observed in semiconductor quantum dots where nanoparticle crystal radius is at the same level as the exciton radius.

2.5.3 Tunable photoluminescent properties

Photoluminescence refers to the emission of light triggered by absorption of photon by the charge carriers on the surface of a particle. When the energy of an incoming photon is higher than the bandgap energy, it excites the semiconductor particle, which can be described by the semiconductor Bloch equations (SBE) (Lindberg & Koch, 1988).

There are two forms of photoluminescence: fluorescence and phosphorescence. In both processes, incident light (or photon) is absorbed and then larger wavelength light is emitted afterward. But the fundamental difference between the two lies in the time a particle takes to emit light. In case of fluorescence, the light is immediately emitted, while in phosphorescence the material stores the energy for a while and emits light later as some sort of afterglow. At the quantum level, for both of these phenomena, photon must be absorbed and electron in the outer shell must reach an excited state with added energy from a ground state. However, this excited state is unstable and the electron must get back to the ground state following some relaxation steps and hence release energy as higher wavelength light. For fluorescence, this step down of energy happens through a combination of some nonradiative vibrational relaxation and internal conversion until the first excited state or singlet. From there, a light-emitting transition pulls the energy level down to the ground state. The key factor here is that the spin of the electron is maintained and does not affect the process. However, for phosphorescence, electron spin is altered when an intersystem crossing occurs from the singlet state to an energetically favorable triplet state. Electron spin is altered again when the energy level drops to the ground state finally by radiative phosphorescence.

Unlike bulk materials where bandgap is fixed, at nanoscale minimum excitation energy and hence the emission spectra are highly dependent on the size of the particle due to the quantum confinement. Therefore, photoluminescent properties of such particles can be controlled by tuning their morphology. Further tuning of emission and electromagnetic properties is possible by adding suitable dopant. There has been extensive work on characterizing luminescent properties through both theoretical and experimental studies of atomistic processes (Gu et al., 2003; Henglein, 1989; Zwijnenburg, 2012). The size dependence can be characterized by different optical spectroscopic methods to study the absorption and emission spectra as a function of the wavelength of the incident photon.

2.5.4 Properties of silicon nanoparticles

Silicon (Si) is the most widely used semiconductor material with a bulk-scale indirect bandgap of 1.1 eV. Though, there are some allotropic structures of Si that exhibit direct bandgap (Kůsová et al., 2014). Crystal structure of Si is face-centered cubic. Quantum yield and hence the optoelectronic properties of Si at nanoscale can be enhanced up to the standard of a direct bandgap bulk or nanostructured semiconductor just by controlling its morphology and dimension because of the quantum confinement. Size dependence of the photoluminescence of Si nanoparticles at room temperature is illustrated by Meier, Gondorf, Lüttjohann, Lorke, and Wiggers (2007). They also discuss the light-scattering methods in order to harness insights about the electronic recombination dynamics. Because of the tunable luminescent properties, reactivity of the nanocrystal surface, and biocompatibility, silicon quantum dots are good candidates to be used for biomedical diagnosis, imaging, labeling, and probing indicator molecules on cell surfaces. Moreover, porous particles can accommodate drugs and therefore be used as drug carriers. In vivo toxicity of carefully synthesized Si quantum dots is very low, reportedly more than 10 times less than that of CdSe quantum dots while exposed to UV light (Fan & Chu, 2010). However, no in vitro cytotoxic behavior has been reported along with other group IV semiconductors, making them better choice over metal nanoparticles.

2.5.5 Properties of germanium nanoparticles

Germanium (Ge) is the second most popular indirect bandgap (0.66 eV at bulk scale) semiconductor in group IV widely used in microelectronic applications. Generally, Ge nanoparticles are grayish black powder with an average size of 70–120 nm. Usually, Ge is found in diamond crystal structure, which may vary in a cluster of more than 40 atoms. Mechanical stability of Ge clusters is dependent on the crystal structure as reported by Pizzagalli, Galli, Klepeis, and Gygi (2001). Compared to Si, Ge has higher value of static dielectric constant and smaller effective mass of electron-hole pair. Also, electrochemical etching of Ge has not been that successful yet compared to Si. Emission spectrum of Ge particles can be fine-tuned to narrow lines by size purification and leveraging differential surface polarity at nanoscale (Shirahata, Hirakawa, Masuda, & Sakka, 2013).

2.5.6 Properties of zinc sulfide nanoparticles

Zinc sulfide (ZnS) is one of the oldest inorganic semiconductor materials occurring in different minerals in nature. It is commonly used as white pigment. Moreover, it can be extracted as by-product of ammonia synthesis. It is a well-known phosphor with a bandgap of 3.67 eV, popularly used in manufacturing display. Nanoparticles of ZnS are found as polymorphic crystal structures. Two major structures are hexagonal and cubic (i.e., wurtzite and sphalerite, respectively). They have excellent chemical resistance against oxidation and hydrolysis. Moreover, they manifest zero toxicity and superior catalytic properties that can be utilized for environmental protection. Luminescent property of ZnS particles enables them to detect alpha-rays. Their infrared optical properties can be used to build optical equipment (i.e., lens, microscopes). They also exhibit phosphor property that is utilized in X-ray screens as well as in cathode ray tubes.

2.5.7 Properties of zinc oxide nanoparticles

Zinc sulfide (ZnO) is a popular semiconductor nanomaterial with a direct bandgap of 3.37 eV at bulk scale (Li et al., 1996). Nanoscaled ZnO particles are considered one of the most commonly used and industrially produced nanoparticles. Their properties are subject to particle size and method of synthesis (Mia, Pervez, et al., 2017; Mia, Rana, et al., 2017; Mia et al., 2020; Pervez et al., 2018). In general, diameters of spherical ZnO nanoparticles are smaller than 100 nm. They are transparent to visible light, but absorb UV-ray effectively. This optical behavior makes them popular in manufacturing sunscreen. Furthermore, they show biocompatibility and antimicrobial properties. As they do not take part in any toxic reaction with food and nutrients and have no disagreeable taste or smell, they can be used as preservative, medicine, or antimicrobial agent (Siddiqi, ur Rahman, Tajuddin, & Husen, 2018).

2.5.8 Properties of cadmium sulfide nanoparticles

Cadmium sulfide (CdS) is a direct bandgap semiconductor with a bandgap value of 2.42 eV at bulk scale. As nanoparticles, they are generally yellow (occasionally brown) powder found in nature as either of the two piezoelectric polymorphs: greenockite and hawleyite with hexagonal and cubic crystal structures, respectively. Due to the photoconductivity (i.e., increased conductivity in the presence of light), they are widely used as photoresistors. Moreover, because of the photovoltaic property, they are used in solar cell cores along mixed with p-type semiconductors.

2.5.9 Properties of cadmium selenide nanoparticles

Cadmium selenide (CdSe) is a black to red-black solid inorganic compound belonging to II–VI semiconductor group. At room temperature, it has a bulk direct bandgap of 1.74 eV, which falls in the visible spectrum. In nature, CdSe occurs in either hexagonal (wurtzite) or cubic (sphalerite, rock-salt) crystal structure. At nanoscale, optical and

electrical properties of CdSe can be fine-tuned leveraging the quantum confinement, which results in its application in solar cells, bio-imaging, bifluorescent tagging, electroluminescent devices (i.e., LEDs), and so on. Zero-dimensional CdSe quantum dots are being continuously investigated as a promising material in nanoengineering. Stability and solubility of such quantum dots are dictated by the nature of the ligand shells that encapsulate them.

2.5.10 Properties of cadmium telluride nanoparticles

Cadmium telluride (CdTe) is a group II-VI semiconductor compound with a bulk direct bandgap of 1.5 eV, which falls in the infrared region. However, when it is downsized to a few nanometers in all dimensions, hence turned into a quantum dot, the fluorescence peak then shifts toward the UV region of the spectrum. High absorbance of CdTe quantum dots is reported at that region, which decreases with increased wavelength, and eventually at 470 nm, there is no absorbance at all (Kadim, 2020). Due to efficient photoluminescence property, CdTe quantum dots are used in biological labeling and imaging applications. Low-cost p-n-type thin solar photovoltaic cells can be built by forming a CdTe-CdS sandwich.

2.5.11 Properties of gallium arsenide nanoparticles

Gallium arsenide (GaAs), a group III–V compound, is the second most common semiconductor material after silicon. Unlike silicon, GaAs has a direct bandgap of 1.4–1.45 eV at bulk scale, which makes it more suitable than silicon for highly efficient light emission. This bandgap falls in the infrared region, making it a great substrate to make infrared LEDs, near infrared LDs. Morphologically, it generally has gray cubic zinc blende (ZB) crystal structure. Due to high electrical resistivity and high dielectric constant, GaAs nanoparticles provide better isolation between devices and circuits. Therefore, GaAs particles are more advantageous over Si for manufacturing integrated circuits. Moreover, higher electron mobility of GaAs is used in transistors for wireless communications and high-efficiency photovoltaic cells.

2.5.12 Properties of magnesium oxide nanoparticles

Magnesium oxide (MgO) is a naturally occurring mineral (also known as periclase) that can be extracted by calcination of hydroxides and carbonates of magnesium. As nanoparticles, they are usually white powder, but can be brown or black depending on the presence of foreign elements. Ideally, they have simple rock-salt crystal structure. Mechanical hardness of MgO is very high. When doped with MgO nanoparticles, ceramics undergo grain growth and significant enhancement in fracture toughness (Tan et al., 2013). Optical properties of MgO nanoparticles are dependent on the particle size. Stankic et al. present the optical properties of MgO nanocubes using UV diffuse reflectance spectroscopy (Stankic et al., 2005). They report trends of absorption spectrum as a function of edge length of cubic particles. Because of the superior refractory property, MgO nanoparticles are used as protective coating in plasma

displays. Electron bandgap of MgO is as wide as 7.8 eV, and it has the highest volume resistivity of 1017 Ω m among oxide nanoparticles. Depending on the chemical purity, dielectric constant of MgO ranges from 3.2 to 9.8 at room temperature (Hornak et al., 2018). Because of the dielectric properties of MgO nanoparticles, they perform well as electrical insulators. Chemical properties of MgO nanoparticles are influenced by the temperature and medium of calcination. In general, MgO particles are odorless and nontoxic. They work as good absorbents of toxic ions from aqueous solutions (Hoque et al., 2018; Rahman, Hoque, Rahman, Azmi, et al., 2019; Rahman, Hoque, Rahman, Gafur, et al., 2019a, 2019b). Moreover, their catalytic behavior can be utilized by using them as chemical additive. They also show dehydrating properties at high temperature, inhibit corrosion, and purify water by inhibiting bacterial growth. At low concentration, a pronounced antibacterial activity of MgO is reported at nanoscale, which makes it a potential plant pathogenic antibacterial agent for controlling plant diseases (Cai et al., 2018).

2.5.13 Properties of gallium nitride nanoparticles

Gallium nitride (GaN) is a group III–V semiconductor compound with a wide bulk direct bandgap of 3.4 eV. It has a hexagonal (wurtzite) single crystal structure, but at nanoscale, it can be synthesized in different morphological assemblies (i.e., nanoparticles, nanorods, nanotubes, nanowires, etc.) using varying synthesis techniques. GaN particles have very high mechanical hardness and superior thermal and optical properties that are dependent on the nanocrystal size due to the quantum confinement. Leveraging the tunable optical and dielectric properties, GaN nanostructures are used in a wide range of devices such as LEDs, LDs (laser diodes), biosensors, solar cells, field-effect transistors, photocatalyst for water splitting, piezoelectric nanogenerators, etc. (Lan et al., 2016).

2.5.14 Properties of gallium phosphide nanoparticles

Gallium phosphide (GaP) is a group III–V semiconductor compound with a bulk indirect bandgap of 2.24 eV at room temperature. It generally has cubic zinc blende (ZB) crystal structure. Optical absorption and fluorescence spectra of GaP nanoparticles are reported to be ranging from 200 to 800 nm and 300 to 650 nm, respectively. The quantum confinement at nanoscale allows GaP to exhibit multiple emission bands depending on particle size in the visible light region of the spectrum (Murugan, Miran, Masuda, Lee, & Okamoto, 2018). Therefore, they are widely used as substrate for low-cost red, orange, and green LEDs.

2.5.15 Properties of indium phosphide nanoparticles

Indium phosphide (InP) is another direct bandgap semiconducting compound with bulk bandgaps of 1.42 eV and 1.35 eV in its hexagonal (wurtzite) and cubic (zinc blende) crystal forms, respectively. It exhibit even higher electron mobility than GaAs, making it a potential candidate for using in high-speed optoelectronic devices and digital circuits (Zafar & Iqbal, 2016). Moreover, owing to the comparatively

lower toxicity of InP quantum dots, they are reported to have potential to be a future competitor of cadmium-based quantum dots in terms of luminescence efficiency (Brichkin, 2015).

2.5.16 Properties of indium arsenide nanoparticles

Indium arsenide (InAs) is one of the least widely used group III-V semiconductor compounds with a direct bandgap of approximately 0.354 eV. It occurs as gray crystals with cubic (zinc blende) structure. Properties of InAs are similar to GaAs, and they are very often used together with InP for the maximum utilization of their narrow bandgap and high electron mobility. InAs is widely used as photodiodes to construct infrared detectors and diode lasers. However, both InAs and GaAs are reported to be acutely toxic toward microorganisms (Nguyen, Field, & Sierra-Alvarez, 2020).

2.5.17 Properties of semiconducting nanoshells

Nanoshells are reported to exhibit better luminescence quantum yield compared to single semiconductor particles. Also, the tunability of other optical properties such a as absorbance and scattering is improved by varying the shell material and thickness along with the core morphology (Nayak et al., 2017).

2.6 Properties of carbon-based nanoparticles

Prevalence in nature as numerous allotropes, low cellular toxicity, flexible engineering, and superior physical properties at atomic scale have made carbon-based particles extremely promising in nanotechnology. They are often used together with polymer materials and nanocomposites in order to incorporate their extraordinary electrical conductivity, strong anisotropic thermal conductivity, and mechanical stability (Parvej, Khan, & Hossain, 2022). Due to the allotropic property, many unique structures can be naturally extracted and artificially engineered. Among them, we discuss some of the most widely known nanoparticles below. Fig. 2.8 illustrates some of the

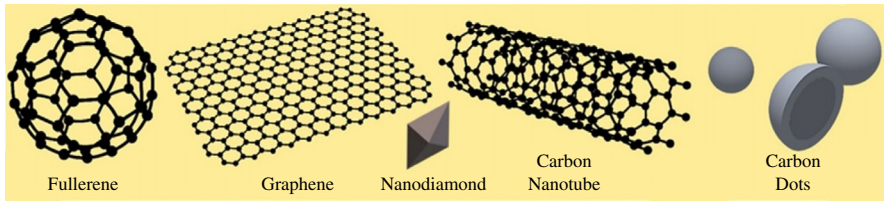

Fig. 2.8 Some of the most popular carbon-based nanomaterials.
Reproduced with permission from Eivazzadeh-Keihan, R., Maleki, A., de la Guardia, M., Bani, M. S., Chenab, K. K., Pashazadeh-Panahi, P., et al. (2019). Carbon based nanomaterials for tissue engineering of bone: Building new bone on small black scaffolds: A review. *Journal of Advanced Research*, *18*(March), 185–201. https://doi.org/10.1016/j.jare.2019.03.011.

most widely known nanoparticles reproduced from Eivazzadeh-Keihan et al. (2019) who discuss them in light of their application in tissue engineering.

2.6.1 Properties of nanodiamonds

Diamonds are one of the most widely known allotropes of carbon where the atoms are arranged in a face-centered cubic crystal structure. Very stable and strong network of hexagonal carbon rings in the structure makes diamonds one of the strongest substances available. Other superlative properties of diamonds include extreme hardness, very high thermal and electrical conductivities, lipophilic (combines with oil, fat, etc.) and hydrophobic (does not get wet by water) nature of its surface, chemical inertness even against strong acids and bases, high value of refractive index, and so on. Nanoscaled diamond particles (nanodiamonds or NDs) are used in myriad of applications such as engine oil additives in order to improve lubrication, high-performance nano-mechanical sensors, nano-electro-mechanical systems (NEMS), in optical and quantum computing, etc. In a comparative study on the cytotoxicity, nanodiamonds have been reported to be the least toxic and most biocompatible among the carbon-based nanoparticles (Schrand et al., 2007). This is why nanodiamonds are used as costly yet very effective therapeutic carrier and catalytic agent. Moreover in bioimaging, labeling, and molecule tracking applications, nanodiamond-based fluorescent probes emit light at 550–800 nm, which makes them advantageous over typical probes emitting light at 400–550 nm. Such probes can be engineered by adsorbing fluorophores or creating nitrogen-vacancy (NV) centers as reported by Mochalin, Shenderova, Ho, and Gogotsi (2012).

2.6.2 Properties of graphene

Graphene is formed with a single layer of the popular carbon allotrope, graphite, comprising a hexagonal honeycomb-like lattice structure of carbon atoms. It exhibits excellent thermal and electrical conductivities, optical transparency, high 2D surface area, and very high mechanical strength. In fact, graphene is the strongest material ever discovered with tensile strength of approximately 130 GPa. Yet, it is extremely thin with only one atom thickness and so light that a single graphene sheet weighing less than a gram is sufficient to cover an entire football field. Optical transparency of graphene is a linear function of the number of layers with each layer absorbing 2.3% of the white light. Therefore, a single layer is approximately 97.7% transparent, while 10 layers would have it reduced to 76%–77% taking into account a very small amount of reflection. Moreover, graphene is capable of absorbing a wide range of electromagnetic radiations and emitting light when excited by near-infrared laser photon, even though it is incapable of forming a released energy state because of zero bandgap (Falkovsky, 2008). Graphene is one of the most promising nanomaterials with applications in drug delivery, cancer therapy, tissue engineering, gene delivery, biomedical sensing devices, etc.

2.6.3 Properties of fullerenes

Fullerenes are carbon molecules having zero-dimensional sp-bonded spherical close-caged structures. The most widely investigated molecule of this group is scientifically named as "buckminsterfullerene" (C_{60}) from which the word "fullerene" originates from. C_{60} molecule is about 1 nm in diameter with strong rotational symmetry. Even though pristine C_{60} is hydrophobic in nature, it is the only carbon-based nanoparticle soluble in organic solvents. In solid crystal form, it is yellow and the organic solution usually turns purple, violet, or wine red. Photochemical activity, optical absorption and fluorescence in the UV and visible light region (Catalan & Elguero, 1993), and antimicrobial activity are reported in recent research (Goodarzi, Da Ros, Conde, Sefat, & Mozafari, 2017). Due to the electron deficiency and reactive exterior, surface-functionalized fullerenes have potential applications in optoelectronics, biomedical drug delivery, and cosmetics. Fullerenes are, in general, not self-inflammable and environmentally nondegradable, but their toxicity has not yet been properly explored.

2.6.4 Properties of carbon nanotubes

Carbon nanotube (CNT) comprises a single sheet of pure graphite rolled to form a cylindrical structure of allotropic carbon network. CNTs are reported to have enhanced properties. Exceptionally high surface area of CNTs along with the capability of chemical attachment with the sidewall of the tube makes them effective in catalytic activity. There are two major types of nanotube structures: single-walled nanotubes (SWNT) and multiwalled nanotubes (MWNT). Single-walled structure has only one rolled layer of hexagonal lattice with a diameter of less than 1 nm, whereas multiwalled nanotubes consist of multiple interlinked layers where the overall diameter can be more than 100 nm. Double-walled nanotubes are one of the common MWNTs exhibiting properties that are similar as SWNTs but having significantly improved resistance to chemicals. Electrical conductivity of CNTs depends on the degree of twist (also known as chirality (Liu, Dobrinsky, & Yakobson, 2010)) of the graphite sheet. SWNTs are reported to be the most electrically conductive carbon fiber, while the conductivity of MWNTs is complex due to the interwall interaction among individual tubes (Kaushik & Majumder, 2015). Due to the strong covalent bond between carbon atoms, Young's elastic modulus of SWNTs can be even higher than 1TPa, while in case of MWNTs, it depends on the amount of disorder in the nanotube wall. Because of the same bond strength, they show superconductivity below 20 K. However, at room temperature, thermal conductivity of nanotubes has been theoretically predicted to be up to 6000 $Wm^{-1}K^{-1}$. Such superior thermal property can be incorporated into nanofluids, which reportedly improves the convection procedure (Khan, Rabbi, Khan, & Mamun, 2016). Capacitance of CNTs is also superior; to scale, it is approximately 1000 times compared to that of regular copper. Moreover, CNTs are strong electron field emitter and good chemical absorbent, and they show superior optical and chemical characteristics. Strength, flexibility, and biocompatibility of CNTs make them capable of controlling and carrying other nanostructures inside

human body; hence, they can be used in medical applications (Eatemadi et al., 2014). Toxicological effects of CNTs are dependent on many factors, most importantly on the morphology. On top of everything, being a carbon-based element, CNTs have almost no environmental impact, rendering it one of the most promising nanomaterials currently.

2.6.5 Properties of carbon nanofibers

Carbon nanofiber (CNF) is produced when graphene sheets are arranged as stacked cones, cups, or plates instead of rolled CNT. CNFs are of low cost and thereby very popular as additives to composite materials as well as in therapeutic drug delivery because of its superior physical properties (Biswas, Chowdhury, Hossain, & Hossain, 2022). It exhibits great mechanical strength (very high tensile modulus), thermal conductivity ($\sim 2000\,\mathrm{Wm^{-1}K^{-1}}$) and electrical conductivity (graphite-like resistivity of only $5 \times 10^{-7}\,\Omega\mathrm{m}$), and electromagnetic shielding property. Binding capacity of CNFs is improved by applying metallic intermediate layers in between two graphene sheets in order to suit them to form high-performance composite materials having applications in nanodevices and structural reinforcement.

2.6.6 Properties of carbon black

Carbon black is a spherical-shaped amorphous carbon material produced by incomplete combustion of petroleum at high temperature (1300°C). Due to the strong adsorption property, major applications of this black fine nanopowder include reinforcing filler rubber products (i.e., tires) and electronic coating. Carbon color also exhibits good tint property that makes it suitable as pigments such as ink, printer toner, paints, varnishes, beauty products such as mascara, etc. Conductive carbon black is often added with other elements to decrease electric resistance. Also due to the UV absorption property, it is used as protective coating to prevent UV degradation of materials. While not mixed with other particles, carbon black is environment-friendly, heat stable, and not self-inflammable.

2.6.7 Properties of carbon dots

Carbon dots are one-dimensional fluorescent nanoparticles. They are important mostly because of their favorable optical behavior. Carbon dots absorb relatively long-wavelength lights peaking in the UV region (250–350 nm) extending to a weak tail in the visible range. They exhibit tunable emission triggered by light, chemical reaction, or electrochemical activity (Bhartiya et al., 2016). Such fluorescence can be controlled and improved in accordance with the application by initial precursor, surface passivation, and synthesis methodology. Due to low toxicity and biocompatibility they have applications in bioimaging, biosensing, drug delivery, catalysis, optical nanoprobes, energy conversion, reinforcement, and UV degradation.

2.7 Properties of ceramic nanoparticles

Ceramic nanoparticles exhibit enhanced mechanical strength, thermochemical stability, and high resistance to environmental changes. One notable concern against the popularity of ceramic nanoparticles is the potential toxicity they may cause in biomedical applications such as drug delivery.

2.7.1 Properties of silicon nitride nanoparticles

There are several types of silicon nitrides (Si_3N_4) developed as engineering ceramics such as reaction-bonded silicon nitride (RBSN), hot-pressed silicon nitride (HPSN), sintered silicon nitride (SSN), sintered reaction-bonded silicon nitride (SRBSN), etc. This material is popular as a nanoceramic particularly because of its superior mechanical properties along with thermochemical stability. At nanoscale, they are silver powder with large spherical surface area. They are capable of resisting oxidation at high temperature, withstanding corrosion, wear, and shock. They do not dissolve in water.

2.7.2 Properties of silicon carbide nanoparticles

Silicon carbide (SiC) is one of the most common ceramic nanoparticles with diverse engineering applications. They are, in general, grayish white powder with high spherical surface area and cubic crystal structure. Similar to silicon nitride, they are also chemically stable and wear resistant. Thermal conductivity of SiC nanoparticles is great, yet expansion in high temperature is favorably low. As composite ceramic, they show dielectric and wave-absorbing properties such as in SiC-SiBCN composite (Ye et al., 2014). Moreover, due to the refractive property, they are good as mirror coating and polishing material.

2.7.3 Properties of nanosilica

Nanoscaled silicon dioxide (SiO_2) particles are commercially referred as nanosilica or silica nanoparticles. Based on structure, there are two types of silica nanoparticles, namely, P-type and S-type nanoparticles, both of which are usually white powder. The key differences between the two types are as follows: P-type particles manifest comparatively higher specific surface area and porosity. They show low toxicity, pozzolanic reactivity, and filler ability as nanopowder (Challa & Das, 2019). P-type silica nanoparticles show high UV reflectivity, making them suitable as protective coating.

2.7.4 Properties of titanium nitride

Titanium nitride (TiN) nanoparticles are mechanically very strong. More specifically, their hardness and wear resistance are remarkable to be used with other ceramics in cutting equipment and bearing materials to enhance life. From transmission electron microscopic (TEM) investigation, TiN nanoparticles are found to be almost spherical

having diameters of roughly 5–20 nm (Zemtsova, Monin, Smirnov, Semenov, & Morozov, 2015). They have high thermal conductivity and high melting point (2950°C), making them capable of withstanding high temperature. Sintering temperature of TiN is so low that they are suitable to be imbedded in nanocomposites. Moreover, they exhibit superior UV-shielding capacity and infrared absorption. Plasmonic performance of single cubic crystal-structured TiN is nearly as good as gold nanoparticles, even though the scattering efficiency is not as high as gold. They also perform well in photocatalytic applications when coated with oxide shells (i.e., TiO_2) (Guler, Suslov, Kildishev, Boltasseva, & Shalaev, 2015).

2.7.5 Properties of alumina

Aluminum oxide or alumina (Al_2O_3) is found in nature in different forms. The most stable form is found in its crystalline as α-Al_2O_3, also known as corundum (polymorphic phase). However, there are some other metastable phases (i.e., cubic, monoclinic, hexagonal, orthorhombic, and tetragonal) (Levin & Brandon, 2005). Superior properties of alumina nanoparticles are exploited in cutting tools, integrated circuits, and in transparent ceramics. They are spherically shaped white powder, while particle size depends on the crystalline structure. Such structures are temperature dependent at a specific particle size, and this dependence is influenced by downsizing of the particles. For instance, the most stable-phased α-alumina stabilizes at a lower temperature at nanoscale. This significantly increases the flexural strength of this nanoceramic (Zemtsova et al., 2015). Alumina particles are highly flammable and show superior dielectric properties and electrical capacity.

2.7.6 Properties of titania

Titanium dioxide or titania (TiO_2) nanoparticles are n-type semiconductor in nature and are found in several polymorphic crystal structures. They can be manufactured in different forms (i.e., powder, crystal, nanorod, tube, and thin film). Titania nanoparticles are very effective yet nontoxic to block UV radiation. On top of that, transparency being their additional feature makes them popular for manufacturing skin-protective cosmetic products such as sunscreens, vanishing cream, beauty creams, etc. They have an additional value in processing ink and as surface coating. Moreover, they show excellent photocatalytic properties (Hossain, Mortuza, et al., 2018; Hossain et al., 2017; Hossain, Pervez, et al., 2018), making them suitable for producing disinfectants and certain antiseptic and antibacterial compounds.

2.7.7 Properties of calcium phosphate

Calcium phosphate (CaP) nanoparticles are available in several forms. The most common forms include tricalcium phosphate ($Ca_3(PO_4)_2$) and hydroxylapatite ($Ca_5(PO_4)_3$). Properties of these nanoparticles depend majorly on the ratio of Ca and P. Because of the biocompatibility and resemblance with the inorganic mineral compositional element in the human skeleton, CaP is a popular choice for bone substitute in medical science. Therefore, as a widely used nonviral vector in the field of

gene therapy, nanoscale CaP can play a vital role in bone tissue engineering through favorable interaction with DNA and RNA (Banik & Basu, 2014). They are structurally spherical of size 10–80 nm with high specific surface area. Solubility of CaP depends on the pH of the environment. Particles dissolving in acidic ($pH < 7$) environment can come in handy in therapeutic drug delivery to subcellular-level organs and tissue. CaP nanoparticles satisfy this requirement at all Ca:P ratios as they become more and more soluble when pH is dropped below 6 (Tabaković, Kester, & Adair, 2012).

2.7.8 Properties of calcium carbonate

Calcium carbonate ($CaCO_3$) is one of the cheapest inorganic materials available as it is abundantly found in nature. Additional advantage includes slow biodegradability. Depending on the synthesis condition, calcium carbonate can be found in three polymorphic crystal structures, namely, calcite (trigonal), aragonite (orthorhombic), and vaterite (hexagonal). Among these, calcite is the most chemically stable form and vaterite is the least stable (Biradar et al., 2011). Nanosized $CaCO_3$ particles are chemically nontoxic and therefore environmentally friendly. Also because of the biocompatibility, they can be used for controlled and nontoxic drug delivery. Recent research in the field of pharmaceutics shows that developing enteric drug delivery system using calcium carbonate is feasible in tablet-encapsulated form (Render et al., 2016). Moreover, they exhibit good radiopaque property.

2.8 Properties of organic nanoparticles

Organic nanomaterials refer to the wide group of nanosized carbon-based compounds directly or indirectly extracted from recently living organisms (i.e., plants and animals) or their waste in environment. This group includes carbohydrates, organic polymers, lipids, proteins, nucleic acids, and any nanostructures associated with these nanomaterials.

Lipids are certain types of hydrocarbons (i.e., fatty acids, glycerolipids, glycerophospholipids, sphingolipids, sterols, prenols, saccharolipids, and polyketides) found in living organisms (Fahy et al., 2009). Lipid-based nanoparticles (LBNP) consist of physiological lipids in different forms. Because of their unique architecture, least amount of toxicity among all types of biocompatible nanoparticles, biodegradability, and capability to dissolve hydrophobic, hydrophilic, and amphiphilic compounds, they are popularly used for nanodrug and associated biomolecular transportation. Many researchers classified these nanoparticles into several types based on their architecture and potential as nanovehicle for biological agents (Chuang, Lin, Huang, & Fang, 2018; García-Pinel et al., 2019).

2.8.1 Properties of liposomes

Liposomes are composed of at least one phospholipid bilayer with an aqueous core as illustrated in Fig. 2.9 (Nagalingam, 2017). One of the major advantages that make them ideal as a nanocarrier for bioactive substances (i.e., drugs, genes) is their

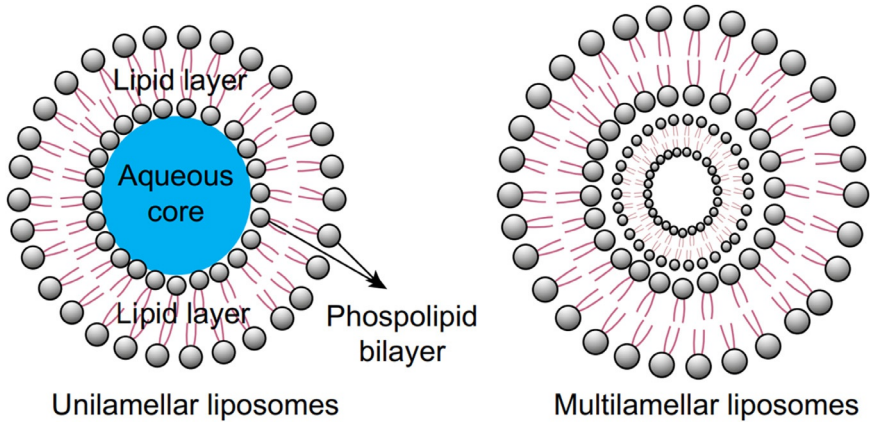

Fig. 2.9 Structure of unilamellar and multilamellar liposomes consisting of phospholipid bilayers with aqueous core.
Reproduced with permission from Nagalingam, A. (2017). Drug delivery aspects of herbal medicines. In *Japanese Kampo medicines for the treatment of common diseases: Focus on inflammation* (pp. 143–164). Elsevier. https://doi.org/10.1016/B978-0-12-809398-6.00015-9.

morphological similarity with cellular membranes. They are also utilized in food industry to preserve sensitive ingredients and enhance performance of food additives.

Different types of liposomes (i.e., multilamellar vesicle, unilamellar vesicle) have different sizes depending on their formation. The diameter of a unilamellar vesicle-type liposome structure can be 50–250 nm, while it is about 1–5 μm for a multilamellar vesicle-type structure (Bozzuto & Molinari, 2015). The core and the lipid bilayer behave differently based on the polarity of the molecules that are targeted to be transported by them. Hydrophilic molecules can be absorbed in the aqueous core, whereas hydrophobic molecules are encapsulated inside the lipid bilayer. Amphiphilic elements are capable of switching their status between both the core and the bilayer, and hence, they can also be carried by liposomes. Moreover, during their synthesis, the fluidity of the lipid bilayer is well moderated to ensure enhanced stability and decreased permeability (Panahi et al., 2017). Permeability of the membrane of phospholipid layer in liposomes is sensitive to temperature. Phase change of phospholipid in liposomes happens at a temperature well below the melting point of phospholipid itself, impacting the stability of the entire structure of liposomes (Panahi et al., 2017).

2.8.2 Properties of lipoprotein

Lipoproteins are naturally occurring lipid-protein complexes consisting of a neutral lipid core made up of cholesteryl esters and triglycerides surrounded by amphipathic lipids or protein molecules. They can be spherical to discoidal in shape with different sizes depending on their density (i.e., protein-to-lipid ratio) ranging from 5 to 1200 nm. They are classified into high-, low-, intermediate-, and very low-density

Table 2.1 Relation between protein density and particle size of different lipoproteins.

Property	HDL	LDL	IDL	VLDL	Chylomicron
Density (g/mL)	1.063–1.210	1.019–1.063	1.006–1.019	0.930–1.006	<0.930
Size (nm)	5–12	18–25	25–35	30–80	75–1200

lipoproteins (HDL, LDL, IDL, and VLDL, respectively) based on their density. If the density goes even below the VLDL, then the particles are called chylomicrons. The denser the complexes, the smaller the size of the particles as presented in the Table 2.1 (Zhang et al., 2011). Behaviors of lipoproteins are dictated by the particle size, structure, and the protein density.

LDLs are naturally found in organisms, whereas HDL can be artificially engineered. So, biocompatibility, nontoxicity, and nonimmunogenic properties are ensured while synthesizing artificial HDL before employing them for cardiovascular treatment (Kornmueller, Vidakovic, & Prassl, 2019).

2.8.3 Properties of lipid-core micelles

Lipid-core micelles are composed of a closed lipid monolayer (fatty acid) in the core coated by a polar surface. Similar to liposomes, lipid-core micelles are spherical in shape. Due to the hydrophobic lipid core, these micelles can effectively carry insoluble and poorly soluble drugs by noninvasive means for the purpose of tumor and cancer treatment (Avasthi & Marshall, 2008).

2.8.4 Properties of hybrid lipid-nanoparticle complexes (HLNC)

Properties of both lipid-based assemblies and inorganic nanoparticles are simultaneously present in these hybrid nanoparticles. HLNCs have been classified into five types in a recent research on their biomedical applications (Vargas, Shon, & Vargas, 2019) based on the localization of the inorganic nanoparticles encapsulated inside the lipid layer. They are listed below along with their corresponding functional properties:

- Liposomes with surface-bound nanoparticles.
- Liposomes with bilayer-embedded nanoparticles.
- Liposomes with core-encapsulated nanoparticles.
- Lipid assemblies with hydrophobic core-encapsulated nanoparticles.
- Lipid bilayer-coated nanoparticles.

2.8.5 Properties of lipoplexes

Lipoplexes or liposome-DNA complexes are nanoparticles comprising one amphiphilic phospholipid bilayer surrounding a hydrophilic core. They are formed as a result of dynamic interaction between positively charged liposomes and negatively

charged plasmid DNA (Ferrari, 2001). Similar to liposomes, they can also be used for transporting bioagents at nanoscale both within its lipid bilayer and within the core. Lipoplexes are spherical in shape. To interpret their morphological structure in detail, two models with fundamental differences have been proposed as follows (Ma, Zhang, Jiang, Zhao, & Lv, 2007):

- External model—DNA is adsorbed (or coated) within the membrane of liposomes.
- Internal model—DNA is surrounded by phospholipid layer.

DNA concentration (i.e., ratio of lipid to DNA) dictates the stability of the structure as well as the zeta potential, which is a parameter representing the surface charge of a particle.

2.8.6 Properties of solid lipid nanoparticles

Solid lipid nanoparticles (SLNs) are one of the most effective colloidal carriers for biocompounds that are primarily composed of lipid matrices (fatty acids, triglycerides, partial glycerides, steroids, waxes, etc.) in solid state at room temperature. They are highly biocompatible and degradable without presenting any threat of toxic by-product. Usually, they are spherical in shape with a diameter of 50–1000 nm. Specific surface area is very high. With proper surface modification, SLN can be used for targeted delivery and controlled release of drugs to treat several chronic diseases as discussed by Ganesan, Ramalingam, Karthivashan, Ko, and Choi (2018). As SLNs are produced in the absence of any toxic organic solvents, safety is ensured in a nanodelivery system.

2.9 Conclusions

This chapter underlines the unique properties of nanoparticles that can be utilized in numerous applications. Exceptional characteristics of nanoparticles are attributed to such quantum confinement and surface effect. More specifically, when the dimension of an object is comparable to the characteristic length of the energy-carrying particles such as electron and photon, they become confined and the properties at such small scale are governed by quantum physics.

Chemical composition of a particle very often dictates its properties. Metallic nanoparticles are particularly popular for their excellent electrical and thermal conductivities along with specific magnetic properties. They exhibit superparamagnetism while downsized below a certain size, which has been briefly discussed. Even though they are the most ancient nanoparticles widely used before as pigments, they are currently one of the most attractive candidates to be used in biomedical applications. Their strong localized SPR allows them to scatter and absorb light in imaging and visualization. Lipid-based organic nanoparticles perform well as vehicle for biological agents due to their structural composition. The biggest forte of semiconductor nanoparticles is their tunable photoluminescence, which is attributed to their widened energy bandgap at nanoscale due to quantum confinement. Ceramic nanoparticles are

mechanically very strong and chemically stable. Different allotropes of carbon with favorable bonding characteristics allow them to form a bunch of nanostructures each having unique properties. However, all of these properties and corresponding nanoparticles can be further explored for more detailed understanding.

References

Alcantara, D., & Josephson, L. (2012). Magnetic nanoparticles for application in biomedical sensing. In *Vol. 4, Issue 1. Frontiers of nanoscience* (1st ed., pp. 269–289). Elsevier Ltd. https://doi.org/10.1016/B978-0-12-415769-9.00011-X.

Anik, M. I., Hossain, M. K., Hossain, I., Ahmed, I., & Doha, R. M. (2021). Biomedical applications of magnetic nanoparticles. In A. Ehrmann, T. A. Nguyen, M. Ahmadi, A. Farmani, & P. Nguyen-Tri (Eds.), *Magnetic nanoparticle-based hybrid materials* (1st ed., pp. 463–497). Sawston, United Kingdom: Elsevier. https://doi.org/10.1016/B978-0-12-823688-8.00002-8.

Anik, M. I., Hossain, M. K., Hossain, I., Mahfuz, A. M. U. B., Rahman, M. T., & Ahmed, I. (2021). Recent progress of magnetic nanoparticles in biomedical applications: A review. *Nano Select*, *2*, 1146–1186. https://doi.org/10.1002/nano.202000162.

Avasthi, P., & Marshall, W. F. (2008). Micelles and nanoparticles for ultrasonic drug and gene delivery. *Advanced Drug Delivery Reviews*, *60*(10), 1137–1152. https://doi.org/10.1016/j.addr.2008.03.008.

Banik, M., & Basu, T. (2014). Calcium phosphate nanoparticles: A study of their synthesis, characterization and mode of interaction with salmon testis DNA. *Dalton Transactions*, *43*(8), 3244–3259. https://doi.org/10.1039/C3DT52522H.

Basher, M. K., Mishan, R., Biswas, S., Hossain, M. K., Akand, M. A. R., & Matin, M. A. (2019). Study and analysis the Cu nanoparticle assisted texturization forming low reflective silicon surface for solar cell application. *AIP Advances*, *9*(7), 075118. https://doi.org/10.1063/1.5109003.

Bhartiya, P., Singh, A., Kumar, H., Jain, T., Singh, B. K., & Dutta, P. K. (2016). Carbon dots: Chemistry, properties and applications. *Journal of the Indian Chemical Society*, *93*(7), 759–766.

Biradar, S., Ravichandran, P., Gopikrishnan, R., Goornavar, V., Hall, J. C., Ramesh, V., et al. (2011). Calcium carbonate nanoparticles: Synthesis, characterization and biocompatibility. *Journal of Nanoscience and Nanotechnology*, *11*(8), 6868–6874. https://doi.org/10.1166/jnn.2011.4251.

Bisht, V., Rajeev, K. P., & Banerjee, S. (2010). Anomalous magnetic behavior of CuO nanoparticles. *Solid State Communications*, *150*(17–18), 884–887. https://doi.org/10.1016/j.ssc.2010.01.048.

Biswas, M. C., Chowdhury, A., Hossain, M. M., & Hossain, M. K. (2022). Applications, drawbacks and future scope of nanoparticles-based polymer composites. In M. R. Sanjay, J. Parameswaranpillai, T. G. Y. Gowda, I. H. S. Siengchin, & M.Ö. Seydibeyoğlu (Eds.), *Met. Nanoparticle-Based Polym. Compos.* (1st Ed.). Elsevier. https://doi.org/10.1016/B978-0-12-824272-8.00002-6.

Bochenkov, V. E., Zagorsky, V. V., & Sergeev, G. B. (2004). Chemiresistive properties of lead nanoparticles, covered by oxide and sulfide layer. *Sensors and Actuators B: Chemical*, *103*(1–2), 375–379. https://doi.org/10.1016/j.snb.2004.04.066.

Bødker, F., Mørup, S., & Linderoth, S. (1994). Surface effects in metallic iron nanoparticles. *Physical Review Letters*, *72*(2), 282–285. https://doi.org/10.1103/PhysRevLett.72.282.

Bozzuto, G., & Molinari, A. (2015). Liposomes as nanomedical devices. *International Journal of Nanomedicine*, *10*, 975. https://doi.org/10.2147/IJN.S68861.

Brichkin, S. B. (2015). Synthesis and properties of colloidal indium phosphide quantum dots. *Colloid Journal*, *77*(4), 393–403. https://doi.org/10.1134/S1061933X15040043.

Brus, L. E. (1983). A simple model for the ionization potential, electron affinity, and aqueous redox potentials of small semiconductor crystallites. *The Journal of Chemical Physics*, *79* (11), 5566–5571. https://doi.org/10.1063/1.445676.

Brus, L. E. (1984). Electron–electron and electron-hole interactions in small semiconductor crystallites: The size dependence of the lowest excited electronic state. *The Journal of Chemical Physics*, *80*(9), 4403–4409. https://doi.org/10.1063/1.447218.

Cahay, M. (2001). *Quantum confinement VI: Nanostructured materials and devices: Proceedings of the international symposium*. The Electrochemical Society.

Cai, L., Chen, J., Liu, Z., Wang, H., Yang, H., & Ding, W. (2018). Magnesium oxide nanoparticles: Effective agricultural antibacterial agent against Ralstonia solanacearum. *Frontiers in Microbiology*, *9*(APR), 1–19. https://doi.org/10.3389/fmicb.2018.00790.

Catalan, J., & Elguero, J. (1993). Fluorescence of fullerenes (C60 and C70). *Journal of the American Chemical Society*, *115*(20), 9249–9252. https://doi.org/10.1021/ja00073a046.

Challa, P. R., & Das, B. B. (2019). *Sustainable construction and building materials*. *Vol. 25* (pp. 397–407). Singapore: Springer. https://doi.org/10.1007/978-981-13-3317-0.

Chuang, S.-Y., Lin, C.-H., Huang, T.-H., & Fang, J.-Y. (2018). Lipid-based nanoparticles as a potential delivery approach in the treatment of rheumatoid arthritis. *Nanomaterials*, *8*(1), 42. https://doi.org/10.3390/nano8010042.

Dahman, Y. (2017). Nanoshells**. By Yaser Dahman, Nabeel Ashfaq, Ahilan Ganesalingam, and Ganeshakumar kobalasingham In *Nanotechnology and functional materials for engineers* (pp. 175–190). Elsevier. https://doi.org/10.1016/B978-0-323-51256-5.00008-3.

Diao, J., Gall, K., & Dunn, M. L. (2003). Surface-stress-induced phase transformation in metal nanowires. *Nature Materials*, *2*(10), 656–660. https://doi.org/10.1038/nmat977.

Dimens, N. (2015). Electrical conductivity of CuO nanofluids. *International Journal of Nano Dimension*, *6*(1), 77–81.

Dolez, P. I. (2015). Nanomaterials definitions, classifications, and applications. In *Nanoengineering* (pp. 3–40). Elsevier. https://doi.org/10.1016/B978-0-444-62747-6.00001-4.

Eatemadi, A., Daraee, H., Karimkhanloo, H., Kouhi, M., Zarghami, N., Akbarzadeh, A., et al. (2014). Carbon nanotubes: Properties, synthesis, purification, and medical applications. *Nanoscale Research Letters*, *9*(1), 393. https://doi.org/10.1186/1556-276X-9-393.

Eivazzadeh-Keihan, R., Maleki, A., de la Guardia, M., Bani, M. S., Chenab, K. K., Pashazadeh-Panahi, P., et al. (2019). Carbon based nanomaterials for tissue engineering of bone: Building new bone on small black scaffolds: A review. *Journal of Advanced Research*, *18* (March), 185–201. https://doi.org/10.1016/j.jare.2019.03.011.

El Badawy, A. M., Silva, R. G., Morris, B., Scheckel, K. G., Suidan, M. T., & Tolaymat, T. M. (2011). Surface charge-dependent toxicity of silver nanoparticles. *Environmental Science & Technology*, *45*(1), 283–287. https://doi.org/10.1021/es1034188.

Elder, A., Yang, H., Gwiazda, R., Teng, X., Thurston, S., He, H., et al. (2007). Testing nanomaterials of unknown toxicity: An example based on platinum nanoparticles of different shapes. *Advanced Materials*, *19*(20), 3124–3129. https://doi.org/10.1002/adma.200701962.

Fahmy, B., & Cormier, S. A. (2009). Copper oxide nanoparticles induce oxidative stress and cytotoxicity in airway epithelial cells. *Toxicology In Vitro*, *23*(7), 1365–1371. https://doi.org/10.1016/j.tiv.2009.08.005.

Fahy, E., Subramaniam, S., Murphy, R. C., Nishijima, M., Raetz, C. R. H., Shimizu, T., et al. (2009). Update of the LIPID MAPS comprehensive classification system for lipids.

Journal of Lipid Research, *50*(Supplement), S9–S14. https://doi.org/10.1194/jlr.R800095-JLR200.

Falkovsky, L. A. (2008). Optical properties of graphene. *Journal of Physics: Conference Series*, *129*, 012004. https://doi.org/10.1088/1742-6596/129/1/012004.

Fan, J., & Chu, P. K. (2010). Group IV nanoparticles: Synthesis, properties, and biological applications. *Small*, *6*(19), 2080–2098. https://doi.org/10.1002/smll.201000543.

Ferrari, M. E. (2001). Trends in lipoplex physical properties dependent on cationic lipid structure, vehicle and complexation procedure do not correlate with biological activity. *Nucleic Acids Research*, *29*(7), 1539–1548. https://doi.org/10.1093/nar/29.7.1539.

Feynmann, R. P. (2018). Feynman and computation. In *Vol. 22*. *Engineering and science* (pp. 22–36). CRC Press. https://doi.org/10.1201/9780429500459.

Ganesan, P., Ramalingam, P., Karthivashan, G., Ko, Y. T., & Choi, D.-K. (2018). Recent developments in solid lipid nanoparticle and surface-modified solid lipid nanoparticle delivery systems for oral delivery of phyto-bioactive compounds in various chronic diseases. *International Journal of Nanomedicine*, *13*, 1569–1583. https://doi.org/10.2147/IJN.S155593.

García-Pinel, B., Porras-Alcalá, C., Ortega-Rodríguez, A., Sarabia, F., Prados, J., Melguizo, C., et al. (2019). Lipid-based nanoparticles: Application and recent advances in cancer treatment. *Nanomaterials*, *9*(4), 638. https://doi.org/10.3390/nano9040638.

Gatoo, M. A., Naseem, S., Arfat, M. Y., Mahmood Dar, A., Qasim, K., & Zubair, S. (2014). Physicochemical properties of nanomaterials: Implication in associated toxic manifestations. *BioMed Research International*, *2014*(August), 1–8. https://doi.org/10.1155/2014/498420.

Goodarzi, S., Da Ros, T., Conde, J., Sefat, F., & Mozafari, M. (2017). Fullerene: Biomedical engineers get to revisit an old friend. *Materials Today*, *20*(8), 460–480. https://doi.org/10.1016/j.mattod.2017.03.017.

Grigore, M., Biscu, E., Holban, A., Gestal, M., & Grumezescu, A. (2016). Methods of synthesis, properties and biomedical applications of CuO nanoparticles. *Pharmaceuticals*, *9*(4), 75. https://doi.org/10.3390/ph9040075.

Gu, F., Wang, S. F., Lü, M. K., Qi, Y. X., Zhou, G. J., Xu, D., et al. (2003). Luminescent properties of Mn^{2+}-doped SnO_2 nanoparticles. *Inorganic Chemistry Communications*, *6*(7), 882–885. https://doi.org/10.1016/S1387-7003(03)00135-7.

Guler, U., Suslov, S., Kildishev, A. V., Boltasseva, A., & Shalaev, V. M. (2015). Colloidal plasmonic titanium nitride nanoparticles: Properties and applications. *Nanophotonics*, *4*(3), 269–276. https://doi.org/10.1515/nanoph-2015-0017.

Henglein, A. (1989). Small-particle research: Physicochemical properties of extremely small colloidal metal and semiconductor particles. *Chemical Reviews*, *89*(8), 1861–1873. https://doi.org/10.1021/cr00098a010.

Hoque, M. A., Ahmed, M. R., Rahman, G. T., Rahman, M. T., Islam, M. A., Khan, M. A., et al. (2018). Fabrication and comparative study of magnetic Fe and α-Fe_2O_3 nanoparticles dispersed hybrid polymer (PVA + Chitosan) novel nanocomposite film. *Results in Physics*, *10*, 434–443. https://doi.org/10.1016/j.rinp.2018.06.010.

Hornak, J., Trnka, P., Kadlec, P., Michal, O., Mentlík, V., Šutta, P., et al. (2018). Magnesium oxide nanoparticles: Dielectric properties, surface functionalization and improvement of epoxy-based composites insulating properties. *Nanomaterials*, *8*(6), 381. https://doi.org/10.3390/nano8060381.

Hossain, M. K., Ahmed, M. H., Khan, M. I., Miah, M. S., & Hossain, S. (2021). Recent progress of rare earth oxides for sensor, detector, and electronic device applications: A review. *ACS Applied Electronic Materials*, *3*, 4255–4283. https://doi.org/10.1021/acsaelm.1c00703.

Hossain, M. K., Hossain, S., Ahmed, M. H., Khan, M. I., Haque, N., & Raihan, G. A. (2021). A review on optical applications, prospects, and challenges of rare-earth oxides. *ACS Applied Electronic Materials*, *3*, 3715–3746. https://doi.org/10.1021/acsaelm.1c00682.

Hossain, M. K., Khan, M. I., & El-Denglawey, A. (2021). A review on biomedical applications, prospects, and challenges of rare earth oxides. *Applied Materials Today*, *24*, 101104. https://doi.org/10.1016/j.apmt.2021.101104.

Hossain, M. K., Mortuza, A. A., Sen, S. K., Basher, M. K., Ashraf, M. W., Tayyaba, S., et al. (2018). A comparative study on the influence of pure anatase and Degussa-P25 TiO_2 nanomaterials on the structural and optical properties of dye sensitized solar cell (DSSC) photoanode. *Optik*, *171*, 507–516. https://doi.org/10.1016/j.ijleo.2018.05.032.

Hossain, M. K., Pervez, M. F., Mia, M. N. H., Mortuza, A. A., Rahaman, M. S., Karim, M. R., et al. (2017). Effect of dye extracting solvents and sensitization time on photovoltaic performance of natural dye sensitized solar cells. *Results in Physics*, *7*, 1516–1523. https://doi.org/10.1016/j.rinp.2017.04.011.

Hossain, M. K., Pervez, M. F., Uddin, M. J., Tayyaba, S., Mia, M. N. H., Bashar, M. S., et al. (2018). Influence of natural dye adsorption on the structural, morphological and optical properties of TiO_2 based photoanode of dye-sensitized solar cell. *Materials Science-Poland*, *36*(1), 93–101. https://doi.org/10.1515/msp-2017-0090.

Hossen, S., Hossain, M. K., Basher, M. K., Mia, M. N. H., Rahman, M. T., & Uddin, M. J. (2019). Smart nanocarrier-based drug delivery systems for cancer therapy and toxicity studies: A review. *Journal of Advanced Research*, *15*, 1–18. https://doi.org/10.1016/j.jare.2018.06.005.

Huber, D. (2005). Synthesis, properties, and applications of iron nanoparticles. *Small*, *1*(5), 482–501. https://doi.org/10.1002/smll.200500006.

Joy, P. A., Kumar, P. S. A., & Date, S. K. (1998). The relationship between field-cooled and zero-field-cooled susceptibilities of some ordered magnetic systems. *Journal of Physics: Condensed Matter*, *10*(48), 11049–11054. https://doi.org/10.1088/0953-8984/10/48/024.

Kadim, A. M. (2020). Applications of cadmium telluride (CdTe) in nanotechnology. In *Nanomaterials—Toxicity, human health and environment* (pp. 1–11). IntechOpen. https://doi.org/10.5772/intechopen.85506.

Kaushik, B. K., & Majumder, M. K. (2015). Carbon nanotube based VLSI interconnects. In *SpringerBriefs in applied sciences and technology* (pp. i–iv). India: Springer. https://doi.org/10.1007/978-81-322-2047-3. Issue 9788132220466.

Khairutdinov, R. F. (1998). Chemistry of semiconductor nanoparticles. *Russian Chemical Reviews*, *67*(2), 109–122. https://doi.org/10.1070/RC1998v067n02ABEH000339.

Khan, M. I., Rabbi, K. M., Khan, S., & Mamun, M. A. H. (2016). Mixed convection analysis in lid-driven cavity with sinusoidally curved bottom wall using CNT-water nanofluid. In *Vol. 1754. AIP conference proceedings* (p. 040015). https://doi.org/10.1063/1.4958375.

Khan, M. I., Hossain, M. I., Hossain, M. K., Rubel, M. H. K., Hossain, K. M., Mahfuz, A. M. U. B., & Anik, M. I. (2022). Recent progress in nanostructured smart drug delivery systems for cancer therapy: A review. *ACS Applied Bio Materials*, *5*, 971–1012. https://doi.org/10.1021/acsabm.2c00002.

Kim, J., & Globerman, S. (2017). Physical distance vs. clustering as influences on contracting complexity for biopharmaceutical alliances. *Industry and Innovation*, *4*, 1–28. https://doi.org/10.1080/13662716.2017.1395730.

Kornmueller, Vidakovic, & Prassl. (2019). Artificial high density lipoprotein nanoparticles in cardiovascular research. *Molecules*, *24*(15), 2829. https://doi.org/10.3390/molecules24152829.

Kosuda, K. M., Bingham, J. M., Wustholz, K. L., & Van Duyne, R. P. (2011). Nanostructures and surface-enhanced Raman spectroscopy. In *Comprehensive nanoscience and technology* (pp. 263–301). Elsevier. https://doi.org/10.1016/B978-0-12-374396-1.00110-0.

Kumar, D. S., Kumar, B. J., & Mahesh, H. M. (2018). Quantum nanostructures (QDs): An overview. In *Synthesis of inorganic nanomaterials* (pp. 59–88). Elsevier.

Kůsová, K., Hapala, P., Valenta, J., Jelínek, P., Cibulka, O., Ondič, L., et al. (2014). Direct bandgap silicon: Tensile-strained silicon nanocrystals. *Advanced Materials Interfaces*, *1* (2), 1300042. https://doi.org/10.1002/admi.201300042.

Lan, Y., Li, J., Wong-Ng, W., Derbeshi, R., Li, J., & Lisfi, A. (2016). Free-standing self-assemblies of gallium nitride nanoparticles: A review. *Micromachines*, *7*(9), 121. https://doi.org/10.3390/mi7090121.

Levin, I., & Brandon, D. (2005). Metastable alumina polymorphs: Crystal structures and transition sequences. *Journal of the American Ceramic Society*, *81*(8), 1995–2012. https://doi.org/10.1111/j.1151-2916.1998.tb02581.x.

Li, S., Silvers, S. J., & Samy El-Shall, M. (1996). Preparation, characterization and optical properties of zinc oxide nanoparticles. *MRS Proceedings*, *452*, 389. https://doi.org/10.1557/PROC-452-389.

Lindberg, M., & Koch, S. W. (1988). Effective Bloch equations for semiconductors. *Physical Review B*, *38*(5), 3342–3350. https://doi.org/10.1103/PhysRevB.38.3342.

Lines, M. G. (2008). Nanomaterials for practical functional uses. *Journal of Alloys and Compounds*, *449*(1–2), 242–245. https://doi.org/10.1016/j.jallcom.2006.02.082.

Liu, Y., Dobrinsky, A., & Yakobson, B. I. (2010). Graphene edge from armchair to zigzag: The origins of nanotube chirality? *Physical Review Letters*, *105*, 235502. https://doi.org/10.1103/PhysRevLett.105.235502.

Liu, Y.-k., Ye, J., Han, Q., Tao, R., Liu, F., & Wang, W. (2015). Toxicity and bioactivity of cobalt nanoparticles on the monocytes. *Orthopaedic Surgery*, *7*(2), 168–173. https://doi.org/10.1111/os.12180.

Loos, M. (2015). Nanoscience and nanotechnology. In *Carbon nanotube reinforced composites* (pp. 1–36). Elsevier. https://doi.org/10.1016/B978-1-4557-3195-4.00001-1.

Ma, B., Zhang, S., Jiang, H., Zhao, B., & Lv, H. (2007). Lipoplex morphologies and their influences on transfection efficiency in gene delivery. *Journal of Controlled Release*, *123*(3), 184–194. https://doi.org/10.1016/j.jconrel.2007.08.022.

Mahfuz, A. M. U., Hossain, M. K., Khan, M. I., Hossain, I., & Anik, M. I. (2022). Smart drug-delivery nanostructured systems for cancer therapy. In Gil Gonçalves (Ed.), *New Trends Smart Nanostructured Biomater. Heal. Sci.* (1st). Elsevier. In press.

Malik, M. A., O'Brien, P., & Revaprasadu, N. (2000). Semiconductor nanoparticles: Their properties, synthesis and potential for application. *South African Journal of Science*, *96*(2), 55–60.

Manzoor, S., Ashraf, M. W., Tayyaba, S., & Hossain, M. K. (2021). Recent progress of fabrication, characterization, and applications of anodic aluminum oxide (AAO) membrane: A review. *arXiv*. http://arxiv.org/abs/2112.08450.

Meier, C., Gondorf, A., Lüttjohann, S., Lorke, A., & Wiggers, H. (2007). Silicon nanoparticles: Absorption, emission, and the nature of the electronic bandgap. *Journal of Applied Physics*, *101*(10), 103112. https://doi.org/10.1063/1.2720095.

Mia, M. N. H., Habiba, U., Pervez, M. F., Kabir, H., Nur, S., Hossen, M. F., et al. (2020). Investigation of aluminum doping on structural and optical characteristics of sol–gel assisted spin-coated nano-structured zinc oxide thin films. *Applied Physics A*, *126*(3), 162. https://doi.org/10.1007/s00339-020-3332-z.

Mia, M. N. H., Pervez, M. F., Hossain, M. K., Rahman, M. R., Uddin, M. J., Al Mashud, M. A., et al. (2017). Influence of Mg content on tailoring optical bandgap of Mg-doped ZnO thin film prepared by sol-gel method. *Results in Physics*, *7*, 2683–2691. https://doi.org/10.1016/j.rinp.2017.07.047.

Mia, N. H., Rana, S. M., Pervez, F., Rahman, M. R., Hossain, K., Mortuza, A. A., et al. (2017). Preparation and spectroscopic analysis of zinc oxide nanorod thin films of different thicknesses. *Materials Science-Poland*, *35*(3), 501–510. https://doi.org/10.1515/msp-2017-0066.

Mochalin, V. N., Shenderova, O., Ho, D., & Gogotsi, Y. (2012). The properties and applications of nanodiamonds. *Nature Nanotechnology*, *7*(1), 11–23. https://doi.org/10.1038/nnano.2011.209.

Murugan, M., Miran, W., Masuda, T., Lee, D. S., & Okamoto, A. (2018). Biosynthesized iron sulfide nanocluster enhanced anodic current generation by sulfate reducing bacteria in microbial fuel cells. *ChemElectroChem*, *5*(24), 4015–4020. https://doi.org/10.1002/celc.201801086.

Nagalingam, A. (2017). Drug delivery aspects of herbal medicines. In *Japanese Kampo medicines for the treatment of common diseases: Focus on inflammation* (pp. 143–164). Elsevier. https://doi.org/10.1016/B978-0-12-809398-6.00015-9.

Nanda, K. K. (2009). Size-dependent melting of nanoparticles: Hundred years of thermodynamic model. *Pramana*, *72*(4), 617–628. https://doi.org/10.1007/s12043-009-0055-2.

Nayak, M. K., Singh, J., Singh, B., Soni, S., Pandey, V. S., & Tyagi, S. (2017). Introduction to semiconductor nanomaterial and its optical and electronics properties. In *Metal semiconductor core-shell nanostructures for energy and environmental applications* (pp. 1–33). Elsevier. https://doi.org/10.1016/B978-0-323-44922-9.00001-6.

Nguyen, C. H., Field, J. A., & Sierra-Alvarez, R. (2020). Microbial toxicity of gallium- and indium-based oxide and arsenide nanoparticles. *Journal of Environmental Science and Health, Part A*, *55*(2), 168–178. https://doi.org/10.1080/10934529.2019.1676065.

Panahi, Y., Farshbaf, M., Mohammadhosseini, M., Mirahadi, M., Khalilov, R., Saghfi, S., et al. (2017). Recent advances on liposomal nanoparticles: Synthesis, characterization and biomedical applications. *Artificial Cells, Nanomedicine, and Biotechnology*, *45*(4), 788–799. https://doi.org/10.1080/21691401.2017.1282496.

Parvej, M. S., Khan, M. I., & Hossain, M. K. (2022). Preparation of nanoparticles-based polymer composites. In M. R. Sanjay, J. Parameswaranpillai, T. G. Y. Gowda, I. H. S. Siengchin, & M.Ö. Seydibeyoğlu (Eds.), *Met. Nanoparticle-Based Polym. Compos.* (1st ed.). Elsevier. https://doi.org/10.1016/B978-0-12-824272-8.00013-0.

Pervez, M. F., Mia, M. N. H., Hossain, S., Saha, S. M. K., Ali, M. H., Sarker, P., et al. (2018). Influence of total absorbed dose of gamma radiation on optical bandgap and structural properties of Mg-doped zinc oxide. *Optik*, *162*, 140–150. https://doi.org/10.1016/j.ijleo.2018.02.063.

Pizzagalli, L., Galli, G., Klepeis, J. E., & Gygi, F. (2001). Structure and stability of germanium nanoparticles. *Physical Review B*, *63*(16), 165324. https://doi.org/10.1103/PhysRevB.63.165324.

Porcel, E., Liehn, S., Remita, H., Usami, N., Kobayashi, K., Furusawa, Y., et al. (2010). Platinum nanoparticles: A promising material for future cancer therapy? *Nanotechnology*, *21*(8), 085103. https://doi.org/10.1088/0957-4484/21/8/085103.

Qi, W. H., & Wang, M. P. (2004). Size and shape dependent melting temperature of metallic nanoparticles. *Materials Chemistry and Physics*, *88*(2–3), 280–284. https://doi.org/10.1016/j.matchemphys.2004.04.026.

Rahman, M. T., Hoque, M. A., Rahman, G. T., Azmi, M. M., Gafur, M. A., Khan, R. A., et al. (2019). Fe_2O_3 nanoparticles dispersed unsaturated polyester resin based nanocomposites: Effect of gamma radiation on mechanical properties. *Radiation Effects and Defects in Solids*, *174*(5–6), 480–493. https://doi.org/10.1080/10420150.2019.1606809.

Rahman, M. T., Hoque, M. A., Rahman, G. T., Gafur, M. A., Khan, R. A., & Hossain, M. K. (2019a). Evaluation of thermal, mechanical, electrical and optical properties of metal-oxide dispersed HDPE nanocomposites. *Materials Research Express*, *6*(8), 085092. https://doi.org/10.1088/2053-1591/ab22d8.

Rahman, M. T., Hoque, M. A., Rahman, G. T., Gafur, M. A., Khan, R. A., & Hossain, M. K. (2019b). Study on the mechanical, electrical and optical properties of metal-oxide nanoparticles dispersed unsaturated polyester resin nanocomposites. *Results in Physics*, *13*, 102264. https://doi.org/10.1016/j.rinp.2019.102264.

Reddington, E., Sapienza, A., Gurau, B., Viswanathan, R., Sarangapani, S., Smotkin, E. S., et al. (1999). Combinatorial electrochemistry: A highly parallel, optical screening method for discovery of better electrocatalysts. *Chemtracts*, *12*(5), 319–321.

Render, D., Samuel, T., King, H., Vig, M., Jeelani, S., Babu, R. J., et al. (2016). Biomaterial-derived calcium carbonate nanoparticles for enteric drug delivery. *Journal of Nanomaterials*, *2016*, 1–8. https://doi.org/10.1155/2016/3170248.

Rubel, M. H. K., & Hossain, M. K. (2022). Crystal structures and properties of nanomagnetic materials. In R. K. Gupta, S. R. Mishra, & T. A. Nguyen (Eds.). *1st. Low Dimens. Magnets*. CRC Press. In press.

Saha, S. M. K., Ali, M. H., Hossen, M. F., Pervez, M. F., Mia, M. N. H., Hossain, M. K., et al. (2018). Structural, morphological, and optical properties of CuO thin films treated by gamma ray. In *2018 international conference on computer, communication, chemical, material and electronic engineering (IC4ME2)* (pp. 1–4). IEEE. https://doi.org/10.1109/IC4ME2.2018.8465649.

Schrand, A. M., Huang, H., Carlson, C., Schlager, J. J., Ōsawa, E., Hussain, S. M., et al. (2007). Are diamond nanoparticles cytotoxic? *The Journal of Physical Chemistry B*, *111*(1), 2–7. https://doi.org/10.1021/jp066387v.

Sharma, P., Ganti, S., & Bhate, N. (2003). Effect of surfaces on the size-dependent elastic state of nano-inhomogeneities. *Applied Physics Letters*, *82*(4), 535–537. https://doi.org/10.1063/1.1539929.

Shirahata, N., Hirakawa, D., Masuda, Y., & Sakka, Y. (2013). Size-dependent color tuning of efficiently luminescent germanium nanoparticles. *Langmuir*, *29*(24), 7401–7410. https://doi.org/10.1021/la303482s.

Siddiqi, K. S., ur Rahman, A., Tajuddin, & Husen, A. (2018). Properties of zinc oxide nanoparticles and their activity against microbes. *Nanoscale Research Letters*, *13*(1), 141. https://doi.org/10.1186/s11671-018-2532-3.

Singh, M., Goyal, M., & Devlal, K. (2018). Size and shape effects on the band gap of semiconductor compound nanomaterials. *Journal of Taibah University for Science*, *12*(4), 470–475. https://doi.org/10.1080/16583655.2018.1473946.

Stankic, S., Müller, M., Diwald, O., Sterrer, M., Knözinger, E., & Bernardi, J. (2005). Size-dependent optical properties of MgO nanocubes. *Angewandte Chemie International Edition*, *44*(31), 4917–4920. https://doi.org/10.1002/anie.200500663.

Stanton, L. (1973). Selection rules for pure rotation and vibration-rotation hyper-Raman spectra. *Journal of Raman Spectroscopy*, *1*(1), 53–70. https://doi.org/10.1002/jrs.1250010105.

Suresh, S. (2013). Semiconductor nanomaterials, methods and applications: A review. *Nanoscience and Nanotechnology*, *3*(3), 62–74. https://doi.org/10.5923/j.nn.20130303.06.

Sweet, M. J., Chessher, A., & Singleton, I. (2012). Review: Metal-based nanoparticles; size, function, and areas for advancement in applied microbiology. *Advances in Applied Microbiology*, *80*, 113–142. https://doi.org/10.1016/B978-0-12-394381-1.00005-2.

Tabaković, A., Kester, M., & Adair, J. H. (2012). Calcium phosphate-based composite nanoparticles in bioimaging and therapeutic delivery applications. *Wiley Interdisciplinary Reviews: Nanomedicine and Nanobiotechnology*, *4*(1), 96–112. https://doi.org/10.1002/wnan.163.

Tan, C. Y., Yaghoubi, A., Ramesh, S., Adzila, S., Purbolaksono, J., Hassan, M. A., et al. (2013). Sintering and mechanical properties of MgO-doped nanocrystalline hydroxyapatite.

Ceramics International, *39*(8), 8979–8983. https://doi.org/10.1016/j.ceramint.2013.04.098.

Temple, T. L., & Bagnall, D. M. (2011). Optical properties of gold and aluminium nanoparticles for silicon solar cell applications. *Journal of Applied Physics*, *109*(8), 084343. https://doi.org/10.1063/1.3574657.

Vargas, K. M., Shon, Y., & Vargas, K. M. (2019). Hybrid lipid–nanoparticle complexes for biomedical applications. *Journal of Materials Chemistry B*, *7*(5), 695–708. https://doi.org/10.1039/C8TB03084G.

Verma, N., & Kumar, N. (2019). Synthesis and biomedical applications of copper oxide nanoparticles: An expanding horizon. *ACS Biomaterials Science & Engineering*, *5*(3), 1170–1188. https://doi.org/10.1021/acsbiomaterials.8b01092.

Wu, Y., Potts, S. E., Hermkens, P. M., Knoops, H. C. M., Roozeboom, F., & Kessels, W. M. M. (2013). Enhanced doping efficiency of Al-doped ZnO by atomic layer deposition using dimethylaluminum isopropoxide as an alternative aluminum precursor. *Chemistry of Materials*, *25*(22), 4619–4622. https://doi.org/10.1021/cm402974j.

Ye, F., Zhang, L., Yin, X., Zhang, Y., Kong, L., Liu, Y., et al. (2014). Dielectric and microwave-absorption properties of SiC nanoparticle/SiBCN composite ceramics. *Journal of the European Ceramic Society*, *34*(2), 205–215. https://doi.org/10.1016/j.jeurceramsoc.2013.08.005.

Yeh, Y.-C., Creran, B., & Rotello, V. M. (2012). Gold nanoparticles: Preparation, properties, and applications in bionanotechnology. *Nanoscale*, *4*(6), 1871–1880. https://doi.org/10.1039/C1NR11188D.

Zafar, F., & Iqbal, A. (2016). Indium phosphide nanowires and their applications in optoelectronic devices. *Proceedings of the Royal Society A: Mathematical, Physical and Engineering Sciences*, *472*(2187), 20150804. https://doi.org/10.1098/rspa.2015.0804.

Zemtsova, E. G., Monin, A. V., Smirnov, V. M., Semenov, B. N., & Morozov, N. F. (2015). Formation and mechanical properties of alumina ceramics based on Al2O3 micro- and nanoparticles. *Physical Mesomechanics*, *18*(2), 134–138. https://doi.org/10.1134/S1029959915020058.

Zhang, X.-F., Liu, Z.-G., Shen, W., & Gurunathan, S. (2016). Silver nanoparticles: Synthesis, characterization, properties, applications, and therapeutic approaches. *International Journal of Molecular Sciences*, *17*(9), 1534. https://doi.org/10.3390/ijms17091534.

Zhang, L., Song, J., Cavigiolio, G., Ishida, B. Y., Zhang, S., Kane, J. P., et al. (2011). Morphology and structure of lipoproteins revealed by an optimized negative-staining protocol of electron microscopy. *Journal of Lipid Research*, *52*(1), 175–184. https://doi.org/10.1194/jlr.D010959.

Zhang, Q., Zhang, K., Xu, D., Yang, G., Huang, H., Nie, F., et al. (2014). CuO nanostructures: Synthesis, characterization, growth mechanisms, fundamental properties, and applications. *Progress in Materials Science*, *60*(1), 208–337. https://doi.org/10.1016/j.pmatsci.2013.09.003.

Zhang, Y., Ding, Z., Zhao, G., Zhang, T., Xu, Q., Cui, B., & Liu, J.-X. (2018). Transcriptional responses and mechanisms of copper nanoparticle toxicology on zebrafish embryos. *J. Hazard. Mater.*, *344*, 1057–1068. https://doi.org/10.1016/j.jhazmat.2017.11.039.

Zwijnenburg, M. A. (2012). Photoluminescence in semiconductor nanoparticles: An atomistic view of excited state relaxation in nanosized ZnS. *Nanoscale*, *4*(12), 3711. https://doi.org/10.1039/c2nr30191a.